UNIVERSITY OF MIAMI

BOUNDARY LAYER, CLOUD, AND DRIZZLE VARIABILITY IN THE SOUTHEAST PACIFIC STRATOCUMULUS REGIME

By

Efthymios Serpetzoglou

A THESIS

Submitted to the Faculty
of the University of Miami
in partial fulfillment of the requirements for
the degree of Master of Science

Coral Gables, Florida

December 2005

UNIVERSITY OF MIAMI

A thesis submitted in partial fulfillment of
the requirements for the degree of
Master of Science

BOUNDARY LAYER, CLOUD, AND DRIZZLE VARIABILITY IN THE SOUTHEAST PACIFIC STRATOCUMULUS REGIME

Efthymios Serpetzoglou

Approved:

_____	_____
Dr. Bruce A. Albrecht Professor of Meteorology	Dr. Steven G. Ullmann Dean of the Graduate School
_____	_____
Dr. Paquita Zuidema Assistant Professor of Meteorology	Dr. Pavlos Kollias Associate Scientist Brookhaven National Laboratory

SERPETZOGLOU, EFTHYMIOS (M.S., Meteorology and Physical Oceanography)
Boundary Layer, Cloud and Drizzle Variability in the Southeast Pacific Stratocumulus Regime (December 2005)

Abstract of a thesis at the University of Miami.

Thesis supervised by Professor Bruce A. Albrecht.
No. of pages in text. (90)

During the past five years, a series of research cruises in the areas of the southeast Pacific stratocumulus regimes have provided unprecedented observations of boundary layer, cloud, and drizzle structures over an area largely unexplored previously. These cruises started with the EPIC 2001 field experiment followed by cruises in a similar area in 2003 and 2004 (PACS/Stratus cruises). The sampling from these three cruises provides a sufficient data set to study the variability occurring over this region. This study compares observations from the 2004 cruise with those obtained during the previous two cruises. Observations on the ship provide information about boundary layer structure, fractional cloudiness, cloud depth, liquid water path, and drizzle characteristics. Our evaluation indicates more strongly decoupled boundary layers during the 2004 cruise than the well-mixed conditions that dominated the cloud and boundary layer structures during the EPIC cruise, and the highly variable conditions – sharp transitions from solid stratus deck to broken-cloud and clear-sky periods – encountered during Stratus 2003. Diurnal forcing and synoptic conditions are being considered as factors affecting these variations. Statistical characteristics of the macrophysical boundary layer and cloud properties are extracted and compared using the 5 to 6-day periods that the research vessels remained stationed at the location of 20°S, 85°W during each cruise. The choice of this domain allows for the elimination of the spatial variability due to different ship

tracks. These results are discussed and summarized and an outlook for future work and research programs is provided.

To the memory of my loved ones:

My grandmother Chrisoula, my grandfathers Kostas and Efthymios

and my aunt Areti

ACKNOWLEDGEMENTS

Several people were instrumental in the completion of this work and the least I can do to show them my appreciation is to acknowledge them.

First of all, I would like to thank my advisor Dr. Bruce Albrecht for offering me the opportunity and ample resources to pursue this research project that included the fascinating experience of participating on field experiments and working with the latest instruments of atmospheric remote sensing. Dr. Albrecht's calm and kind nature in combination with the huge knowledge and experience that he possesses on the field of meteorology have been a constant source of inspiration for me and acted as the catalyst in this process that lead to my personal and academic maturity. I am also indebted to him for his unending guidance, support and understanding that were key factors in the fast and successful completion of this work.

Dr. Pavlos Kollias is another individual that played his own particular role towards the completion of this study. Pavlos not only urged me to make the difficult but yet exciting step of crossing the Atlantic and pursuing my graduate studies at the University of Miami, but has also been helpful and supportive in every aspect ever since. His endless guidance, great ideas and all around help as a member of my committee really made the completion of this project feasible. His expertise on radar meteorology, his ever-growing research interests and his will to share his knowledge and experience with me were extremely influential and motivational towards the accomplishment of my task.

In addition, I would like to express my appreciation to Dr. Paquita Zuidema, who served as member of my committee and improved this thesis substantially through her

helpful inputs and insightful comments. She also provided some of the data used in this study and encouraged me many times by showing great interest in my work. Special thanks are also due to Dr. Christopher Fairall, who is the mastermind of the atmospheric research and field experiments conducted in the Southeast Pacific Stratocumulus Regime. Dr. Fairall kindly provided the majority of the data used in this study and contributed a lot to the organization of the overall project. His great knowledge and humorous side make him a pleasure to work with, and were another source of positive influence and motivation throughout this work. His partner Dan Wolfe also deserves my gratitude not only for the field work that he performed onboard the research vessels, but also due to his constant support, encouragement and companionship both during and after the Stratus 2004 research cruise.

I would also like to thank my radar group mates and friends Virendra Ghate and Ieng Jo for their great friendship and support during these years; Dan Voss for providing continuous and critical computer support; and Tom Snowdon for teaching me a lot about radars. My professors at RSMAS Drs. Nolan, Zhang, Chassignet, Majumdar, Olson, Peters and Leamann are also greatly acknowledged for providing me with the basic scientific tools and background that made me capable of conducting research on the field of meterology.

Moreover, I would like to thank Dr. Christos Mitas for his friendship, his critical help during hurricane Wilma and his constructive comments during the final stages of this work as well as Dr. Villy Kourafalou for her friendship and continuous support during my stay in Miami. Both of them along with Pavlos Kollias made Greece seem much closer than it really was. Marcello, Tania, Manuel (or Dr. Lonfat), Pete and my many

other RSMAS friends have been there for me since the beginning of this new experience, and I really hope that they will be my friends for life.

Last but not least, I would like to thank my parents Iordanis and Sofia and my brother Christos, for their endless love, support and encouragement throughout my entire academic career, and my fiancée, Katerina, for being so patient, loving and encouraging during the last two and a half years that we spent apart. These four people were far away all this time but closer than ever in my mind and heart.

TABLE OF CONTENTS

LIST OF TABLES

LIST OF FIGURES

Chapter 1 – Introduction

1.1 Motivation

During the last two decades, marine stratocumulus clouds have been the center-piece of many theoretical/modeling studies (e.g., Garreaud and Munoz 2004; Bretherton and Wyant 1997) and field experiments (e.g., Albrecht et al. 1988; 1995b). This type of cloud is mainly observed at low levels over the eastern side of the subtropical oceans, where the conditions (cool surface waters – warm, dry air subsiding aloft) favor the creation of a sharp temperature and moisture inversion that caps the Marine Atmospheric Boundary Layer (MABL) and leads to the trapping of the clouds at its top (Klein and Hartmann 1993). Both surface-based cloud climatologies (Klein and Hartmann 1993) and satellite studies (Ramanathan et al. 1989) have clearly indicated the impact of boundary layer clouds on the global radiation budget; their high albedo results in a substantial decrease of the amount of solar radiation reaching the ocean's surface, while their low altitude corresponds to a small temperature difference between cloud-top and the ocean surface that results in little change in thermal radiation emitted to space. Although the role of stratocumulus clouds in affecting the radiation balance by cooling the ocean was recognized through early studies (e.g., Randall et al. 1984), the growing need of a more accurate representation in the Global Climate Models (GCMs) has engaged many scientists in the pursuit of a better understanding of their radiative, microphysical and dynamical properties, the thermodynamic structure of the MABL, and the climatological variability of the respective areas (e.g., Stevens et al. 2003).

One of the most prevalent stratocumulus cloud decks in the world is located over the subtropical southeast Pacific, extending about 1500 km offshore from the Equator to the latitude of central Chile (25-30°S) (Klein and Hartmann 1993). In addition to the large latitudinal extent, the interaction with El Nino-Southern Oscillation (ENSO) and the special morphology of the western South American continent (e.g., the presence of Andes) also contribute to the unique character and high importance of the SE Pacific stratocumulus regime (Li and Philander 1996).

In this study, data collected during three research cruises form the basis for exploring clouds and boundary layer structures in this climate sensitive area. The main objectives are to develop an extensive description of marine stratocumulus macroscopic properties, examine their temporal (diurnal, seasonal and interannual) variability in association with the evolution and variability of the MABL thermodynamic structure, and investigate the effect of large-scale dynamics.

1.2 Background on Climate Research Programs and Field Experiments

The stratus cruises are a very small component of a large ongoing international research effort to better describe, comprehend and predict the world's climate. The international interdisciplinary research program on Climate Variability and Predictability (CLIVAR), under the auspices of the World Climate Research Program (WCRP), investigates the physical and dynamical processes in the climate system that occur on seasonal, interannual, decadal and centennial time-scales. One of the three major CLIVAR science foci is the seasonal-to-interannual variability and predictability of the

Global Ocean-Atmosphere-Land System (GOALS; 1995-2005), which replaced the Tropical Ocean - Global Atmosphere (TOGA) program (1985-1995). CLIVAR is further organized into regional panels, one of which is the Variability of the American Monsoon Systems (VAMOS) that focuses on the climate of the Americas. VAMOS consists of various regionally-oriented science projects; the project currently associated with the SE Pacific area is called VAMOS Ocean-Clouds-Atmosphere-Land Study (VOCALS). The main scientific issues that VOCALS plans to address include: the investigation of the temporal and spatial scales of cloud-topped boundary layer - South American continent interaction; the examination of regional and seasonal/interannual feedbacks between stratocumulus clouds, surface winds, upwelling, coastal currents and Sea Surface Temperature (SST); a focus on feedbacks of SE Pacific cloud-topped boundary layer properties on the overall tropical circulation and ENSO; and the evaluation of the climatic importance of aerosol-cloud interactions. An Intensive Observations Period (IOP) for VOCALS is scheduled for the fall of 2007.

The US CLIVAR office coordinates major participation in this international research effort, being primarily responsible for the climate monitoring programs in the American continent and the surrounding oceans. A major program launched several years ago by US CLIVAR, the Pan-American Climate Studies (PACS), provided the context for more specialized monitoring projects and field experiments on these areas. As a result, the beginning of the 21st century coincided with the first ever US CLIVAR process study: the East Pacific Investigation of Climate (EPIC) processes in the Coupled Ocean-Atmosphere System (1999-2004), which lead to the EPIC 2001 field experiment (Weller 1999). The second leg of the EPIC field campaign was an extensive stratocumulus study

(Bretherton 2004), taking place in October of 2001 and revealing the complex structure of the stratocumulus-topped boundary layer in the subtropical SE Pacific. This first major interdisciplinary field study in the area succeeded in separate significant oceanographic and atmospheric objectives, proved that their combination is crucial to the sustained effort to fully comprehend the ocean-atmosphere-land interactions of the region, and set the path for the SE Pacific field experiments to follow.

An important role in EPIC long-term monitoring is played by the Stratus Ocean Reference Station (Stratus ORS) that was launched in October 2000 at the geographical location of 20°S, 85°W by the Woods Hole Oceanographic Institution (WHOI) Upper Ocean Processes (UOP) group. The recovery and replacement of the Stratus ORS buoy was one of the primary objectives of the EPIC 2001 stratocumulus cruise (hereafter EPIC 2001). Thereafter (with an exception of 2002), the ship campaigns to maintain and replace the buoy have been providing atmospheric researchers with the necessary means to deploy remote sensors and other instrumentation and conduct observations to improve our knowledge of the various processes associated with the SE Pacific stratus deck. The Stratus 2003 (Kollias et al. 2004) and Stratus 2004 (Serpetzoglou et al. 2005) research cruises served as part of the PACS/EPIC enhanced monitoring and process studies implementation schedule, and provided – in combination with EPIC 2001 – a unique data set by capturing most of the properties that are fundamental for studying and analyzing the complex features of stratocumulus clouds and MABL in the subtropical SE Pacific. These measurements also allow stratocumulus in this region to be compared to the better-studied stratocumulus of the Northeast Pacific, and to those sampled in a less instrumented Chilean cruise off of central Chile in October 1999 (Garreaud et al. 2001).

1.3 Scientific Objectives

The main focus of the thesis is to describe the observed variability of stratocumulus properties over the southeast Pacific and improve our understanding of the physical and dynamical processes that lead to the generation, maintenance and dissipation of marine stratocumulus clouds. Under this context, the specific scientific objectives to be addressed in this study are:

I. Compare the evolution of measured and derived MABL and cloud parameters along the three different cruise tracks; describe and explain the associated variability.

II. Extract the climatological means and variances of the basic cloud properties of the subtropical SE Pacific stratus deck as well as the mean profiles of the MABL thermodynamic structure.

Properties such as fractional cloudiness, cloud thickness, drizzle occurrence and liquid water path (LWP) play a substantial role in the lifecycle of marine stratocumulus and their statistical characteristics are essential for realistic climate model simulations. Furthermore, mean profiles of the thermodynamic and dynamical variables (e.g., potential temperature, mixing ratio, wind speed and direction) can provide baseline boundary layer structures for testing models and evaluating the effect that structure may have on boundary layer cloudiness (Albrecht et al. 1995a).

III. Understand and evaluate the observed patterns of mean structure and variability by attempting to isolate some of the physical and dynamical processes that govern the complex ocean-atmosphere coupling in the region and highlight the interconnection between MABL cloud properties, surface meteorology variables and radiative fluxes.

There are still many open issues regarding our understanding of the interactions between the basic features that lead to the generation, maintenance and dissipation of stratocumulus clouds (e.g., Albrecht et al. 1995a). Processes, such as cloud-top radiative cooling, entrainment of dry air above the inversion into the cloud layer, in-cloud circulation and turbulent mixing, and drizzle formation and evaporation beneath the cloud layer interact in a complex manner that makes it difficult to draw final conclusions on the kind and extent of influence that each one individually imposes on the lifecycle of stratus clouds. We attempt to test and evaluate previous assumptions and hypotheses regarding some of these processes.

The role of the large-scale ocean and atmospheric dynamics on influencing the MABL structure and variability is also examined. The Climate Diagnostics Center (CDC) web interactive plots allowed us to obtain the regional SST and Sea Level Pressure (SLP) patterns, the atmospheric pressure systems evolution etc.

Chapter 2 – Data Sets and Analysis Procedures

2.1 Domain Setup

The ship track during each of the three cruises under consideration is shown in Fig. 2.1. Table 2.1 also provides a useful context with respect to significant dates and times of each route. During EPIC 2001 and Stratus 2003, the research vessels followed similar – but not identical – paths, while the Stratus 2004 cruise had a completely different route. The EPIC 2001 cruise started from the Galapagos Islands, where the NOAA research vessel *Ronald H. Brown* (hereafter called the *Brown*) was stationed for a few days following the first leg of the field campaign. From this point, the *Brown* steamed west on October 9 to 95°W and then south along the remainder of the TAO buoy line into the SE Pacific stratocumulus regime. After stopping for approximately 6 days (October 16-22) at the location of the Stratus ORS buoy, the *Brown* reached the port of Arica in northern Chile, on October 25. For Stratus 2003, the UNOLS research vessel *Roger Revelle* (hereafter called the *Revelle*) departed from Manta, Ecuador on November 11. After a short southwesterly course, the ship continued south to reach the WHOI buoy, where it remained for about 5 days (November 15-20). The cruise concluded with a 3-day easterly route to Arica, similar to the *Brown* path during EPIC 2001. For Stratus 2004 however, Arica was the starting point. The *Brown* headed west along the 20°S line, until it reached the Stratus ORS location, where it remained stationed for 5 days as well (December 11-16). After a short westerly route until 90°W, the ship followed a southeasterly route into

the southernmost part of the stratocumulus regime and concluded the trip in Valparaiso, Chile on December 24, after a short southerly transect along the coast of central Chile.

Although the cruise paths followed by the *Brown* in 2001 and 2004 and the *Revelle* in 2003 are quite different in general, there is sufficient overlap in domains for crucial comparisons between the three field experiments. The most important of these domains seems to be the Stratus ORS location (20°S, 85°W), where the ships were stationed for 5 to 6 days on each cruise. This study plans to focus on this location and take advantage of the unique 3-cruise dataset, to study and compare the day-to-day evolution of the cloud-topped boundary layer and attempt to extract the statistical characteristics of the basic cloud properties. The transect along 20°S from 75° to 85° W is also common with all three research cruises, and could be ideal for studying the evolution of the MABL in the transition from the deeper-ocean cold waters to the coastal warmer regime. The temporal lag of the three cruises (October 2001 – November 2003 – December 2004) allows us to extract a monthly variability regarding the afore-mentioned properties, and seek signs of interannual variability, always under the context of the influence of large-scale dynamics.

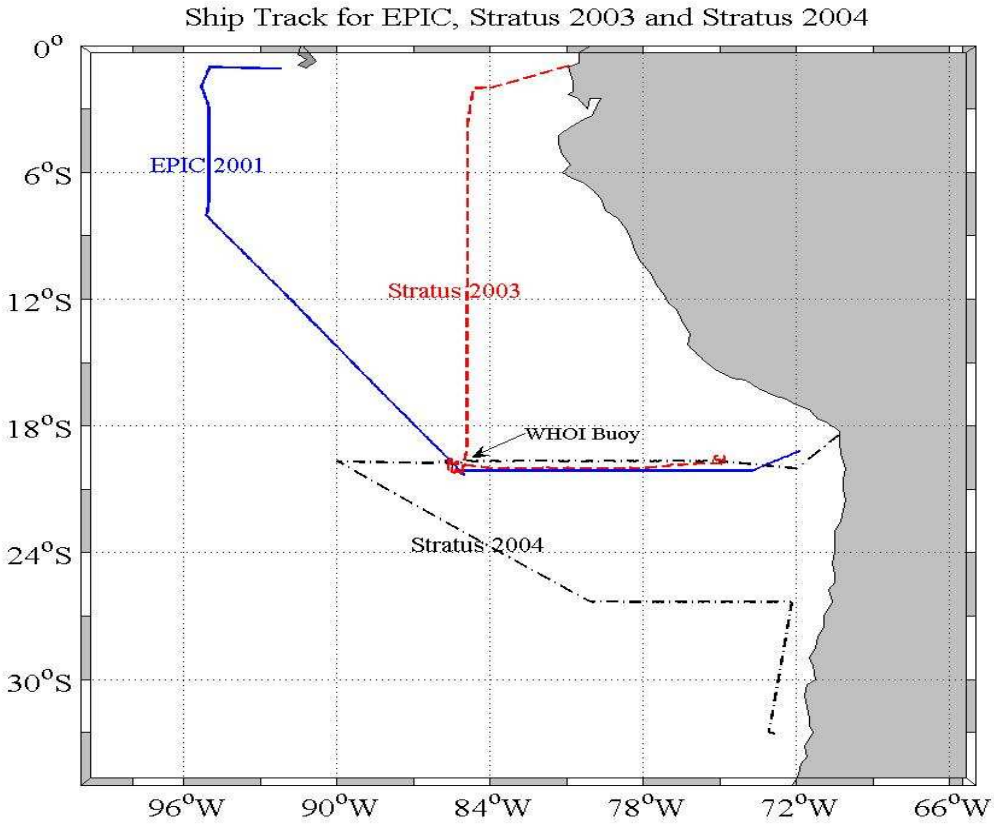

Figure 2.1: The routes that the *Brown* and the *Revelle* followed during EPIC 2001 (blue), Stratus 2003 (red) and Stratus 2004 (black). The arrow points to the location of the Stratus ORS buoy (20°S, 85°W).

Table 2.1: Time schedule for the 3 stratus cruises.

	EPIC 2001	**Stratus 2003**	**Stratus 2004**
Cruise period (dates)	Oct. 9-25	Nov. 11-24	Dec. 5-23
Cruise period (Julian days)	282-298	315-328	340-358
Buoy period (dates)	Oct. 16-22	Nov. 15-21	Dec. 11-16
Buoy period (Julian days)	289-295	319-325	346-351
Exact time of arrival (at the buoy)	(Oct.) 15.955	(Nov.) 15.781	(Dec) 11.181
Exact time of departure	(Oct.) 22.330	(Nov.) 21.375	(Dec.) 16.250

2.2 Instrumentation onboard

The EPIC 2001, Stratus 2003 and Stratus 2004 research cruises were collaborative efforts among various institutions and universities. An extensive suite of instruments was deployed onboard the research vessels for making measurements of boundary layer clouds, thermodynamic structure, surface fluxes and near-surface meteorology. The remote sensors that were used in each cruise and their respective products are briefly described in Table 2.2. All three cruises included a ceilometer, a 3-channel microwave radiometer and an 8.6-mm Doppler cloud radar (although the latter suffered a component failure early in the Stratus 2004 cruise – see section 2.4). Surface meteorology, turbulent and radiative flux measurements (Fairall et al. 1997) as well as aerosol spectrometer measurements provided a near surface complement to these remote sensing instruments. Rawinsondes were also launched during the three field experiments providing a high resolution vertical profile of the MABL thermodynamic structure. During EPIC 2001 the frequency of the sounding launches was relatively high (8 per day), compared with that in Stratus 2003 (4 per day) and Stratus 2004 (4 per day with the exception of 6 per day while at the ORS location). The 2001 and 2004 cruises also included the operation of the C-Band Radar onboard the *Brown* and a 915-MHz wind profiler, while a new very high resolution but low sensitivity 3.2-mm Doppler cloud radar was only used during Stratus 2004.

Table 2.2: A list of the remote sensing instruments onboard the *Brown* and the *Revelle* and the respective products.

Remote Sensor	**Research Cruise**	**Technical Specifications**	**Product**
FMCW* radar	Stratus 2004	94-GHz (3.2 mm) – vertically pointing	First three moments of the Doppler Spectrum
MMCR** pulse radar	All three	35-GHz (8.6 mm) – vertically pointing	First three moments of the Doppler Spectrum
Brown C-Band radar	EPIC 2001, Stratus 2004	5.6-GHz (5.4 cm) – Scanning	Reflectivity and radial velocity
Wind Profiler	EPIC 2001, Stratus 2004	915-MHz (32.8 cm)	Time-height profile of wind speed/direction
Ceilometer	All three	Lidar (Vaisala CT-25K)	Time-height profile of cloud base
Microwave Radiometer	All three	3-channels: 20.6, 31.6, 90 GHz	Column integrated liquid and vapor amounts
* Frequency Modulated Continuous Wave ** Millimeter Cloud Radar			

2.3 Data Availability and Processing

The University of Miami Radar Meteorology Group (UMRMG) participated in the Stratus 2004 experiment and was primarily responsible for the preparation of the deployment, data collection and preliminary processing of the FMCW Doppler cloud radar. We were also actively involved in the operation and data collection of many of the other instruments onboard the *Brown*. Our participation in the cruise provided us with immediate access to the Stratus 2004 data. The data from EPIC 2001 and Stratus 2003 were kindly provided by Dr. Chris Fairall, of the National Oceanic and Atmospheric Administration (NOAA) Earth System Research Laboratory (ESRL) Physical Sciences

Division (PSD) – formerly known as Environmental Technology Laboratory (ETL), – who had the actual command of the atmospheric part in all three cruises.

The first task of this study was to acquire the previously-described data set and perform the necessary quality control. The data collected during EPIC 2001 and Stratus 2003 were provided to us after being subject to a "first-level" processing; the "raw" data files generated directly from each instrumentation system during the collection procedure had been converted to easier-to-read file formats (e.g., text or NetCDF files). We applied similar processing procedures to the "raw" data files obtained during Stratus 2004. All the data from the three cruises were then checked for quality and coherence. The few bugs and errors detected were corrected accordingly. The majority of the data collected during EPIC 2001 and Stratus 2003 did not reveal any particular defects, since they had already been subjected to quality control and processing by the scientists involved in the respective field campaigns.

The unprecedented 3-cruise data set has been the backbone of this study. The choice of the regional domains for the analysis was briefly described and evaluated in section 2.1. Objective I is addressed using cruise-composite time-height cross-sections of the respective properties and profiles. The time period that the ships were stationed at the Stratus ORS location (20°S, 85°W) is used primarily for the accomplishment of objective II, so that the spatial variations associated with the different routes of each cruise are excluded. Emphasis is given to the observed diurnal cycle of some cloud properties, and the possibility of monthly and interannual variability is examined. Composite time-series plots, time-height profiles, histograms etc. are produced and used for the comparison and description of the 3-cruise retrievals of the afore-mentioned properties and features.

Various techniques are used in order to better distinguish between the different MABL structures observed in the SE Pacific stratocumulus regime. For instance, the soundings classification followed by Kloesel and Albrecht (1989) and Yin and Albrecht (2000) is proved very useful for our analysis.

The Vaisala sounding systems (RS-80 sondes in EPIC, RS-90 sondes in Stratus 2003, RS-92 sondes in Stratus 2004) provided profiles of temperature (T), pressure (P), relative humidity (RH), and horizontal wind speed and direction. The data from each of the rawinsonde data sets were then used to calculate potential temperature (θ), virtual potential temperature (θ_v), equivalent- and saturation equivalent potential temperature (θ_e and θ_{es} respectively), and mixing ratio (r). These parameters were calculated using the methods described by Bolton (1980). To obtain an average sounding from each data set for the needs of extracting mean and variance thermodynamic profiles (see Chapter 4), we used two different approaches. The first one included linear interpolation of the initial (raw) sounding data – obtained at variable height levels – to new vertical bins with a height increment of 10 m. Mean and standard deviation values were then calculated for each bin for both measured and derived quantities. This approach allows for an objective quantitative comparison of the vertical MABL profiles sampled during the three cruises, but limits the analysis with respect to the inversion characteristics. To maintain the structure of the inversion in the composite soundings, a non-dimensional height scale was used, following Albrecht et al. (1995a); using this approach, the height (z) is normalized with the inversion base height (z_i) of each sounding to give a nondimensional vertical coordinate z/z_i. The estimation of the inversion base height for each sounding was performed objectively, using the μ parameter described in Yin and Albrecht (2000) (more

elaborate description is provided in section 3.3). Average soundings were then obtained by using vertical bins with a nondimensional height increment of 0.01.

2.4 Technical Difficulties

Since the MMCR component failed on the 4th day of the Stratus 2004 cruise, an alternative way to estimate the cloud-top heights was considered by using the 915 MHz wind-profiler reflectivity. These data provide the inversion height (boundary layer depth) using a technique developed by Chris Fairall and William Otto of NOAA/ETL. The enhanced profiler reflectivity results from Bragg scattering due to the large temperature and moisture jumps that characterize the sharp capping inversion of the SE Pacific boundary layers. This procedure gives an inversion height estimate even if there is no cloud present; but this should not be a major problem, since we are mostly interested in the time-height evolution of cloud top. Moreover, a distinction should be made between the base and the top of the inversion layer. In the presence of stratus clouds the cloud top closely matches the inversion-base height. However, the wind-profiler technique is based on identifying the maximum Bragg scattering resulting from the temperature and moisture inversion jumps, thus giving estimates of cloud-top that lie within the inversion layer and not exactly at the inversion base. This is evident in Fig. 2.2, which shows a comparison of the wind-profiler inversion-height estimates with the heights of the inversion base and inversion top derived from the soundings using the μ-parameter methodology (see section 3.3).

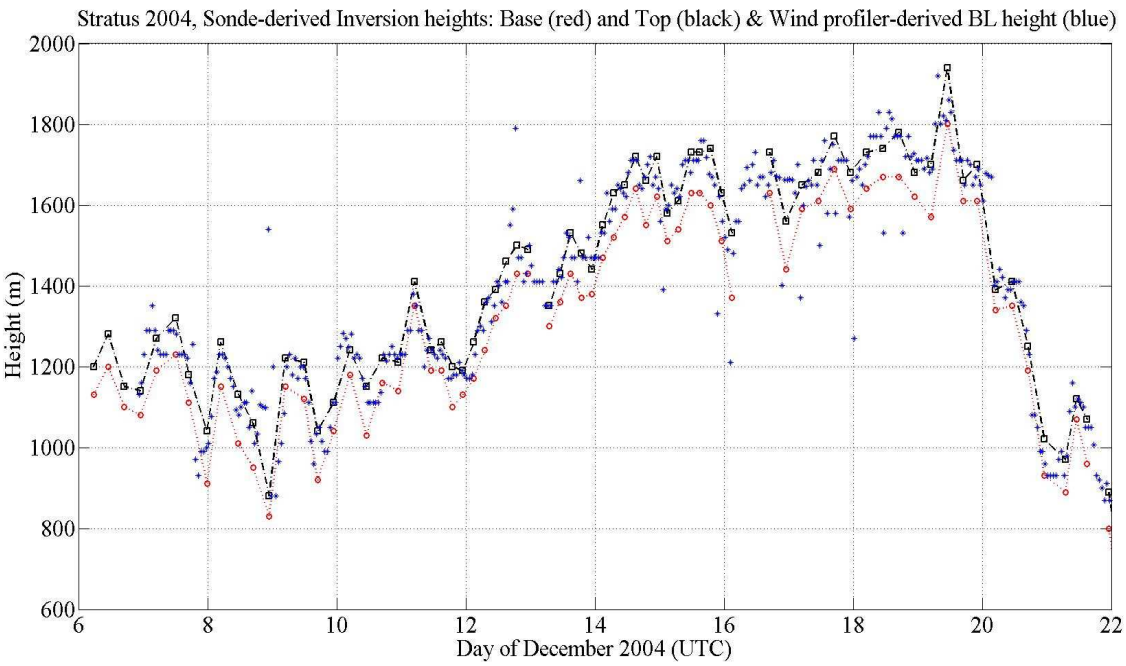

Figure 2.2: Comparison of inversion-top (black squares – dashed-dotted) and inversion-base (red circles – dotted) heights from soundings against wind-profiler-derived BL height (blue stars).

Another instrument problem affects ceilometer data from the Stratus 2004 cruise. The ceilometer appears to have been operating at reduced sensitivity after the 6th day of the cruise. A deterioration of the optical fiber that carries the signal to the detector prevented the instrument of detecting many clouds during daytime when sunlight may contaminate the optical returns (see Appendix, Fig. A1). Fortunately, when clouds are detected, the cloud base height is accurate. After careful examination of all the daily plots of backscatter coefficient and cloud base height, we concluded that the problem is limited between the hours 14:00 and 22:00 UTC (8:00 to 16:00 local time) from December 11 to the end of the cruise. The apparent malfunction does not influence substantially the time-height profile of cloud base, but it makes part of the data unusable with regard to estimating fractional cloudiness and cloud base statistics.

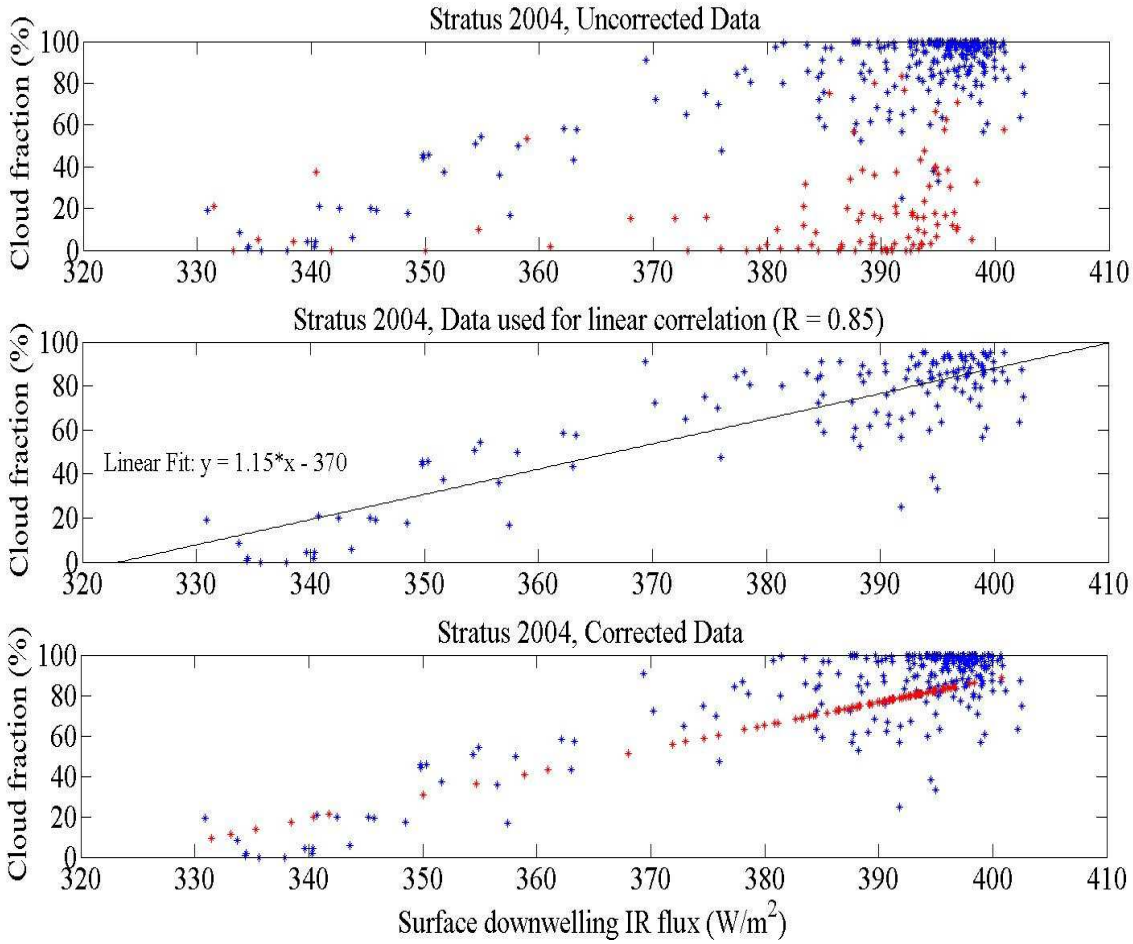

Figure 2.3: Analysis procedure followed for extracting accurate cloud-fraction estimates for the time periods affected by the ceilometer malfunction during Stratus 2004. *Upper panel*: The initial (uncorrected) hourly estimates of ceilometer-derived cloud fraction are plotted against the respective hourly-averaged values of incoming longwave radiation (part of the NOAA/ETL air-sea flux system measurements). Data points corresponding to intervals affected by ceilometer malfunction are marked with red color. *Middle panel*: Same as before, but only including "problem-free" data points with cloud fraction values less than 95%. The linear least-squares fit is plotted with a straight line, and the respective equation and correlation coefficient are also displayed. *Lower panel*: The linear fit is used to estimate the cloud fraction value for the affected data points, identified before (also red colored).

To compensate for the afore-mentioned malfunction and the consequent gap in the daily ceilometer data, incoming longwave radiation is used as a surrogate for fractional cloudiness. Fig. 2.3 represents the analysis procedure followed for making accurate

estimates of the Stratus 2004 cloud fraction. The upper panel of Fig. 2.3 shows the initial (uncorrected) scatterplot between ceilometer-derived hourly cloud-fraction estimates and hourly averages of the downwelling IR flux, as measured by the NOAA/ETL air-sea flux system. The hourly intervals affected by the ceilometer malfunction are plotted with a different color (red), and correspond to data points with high IR flux- (370-400 W/m^2) but low cloud fraction values (lower than 50%). These data points as well as the data points that correspond to cloud fraction values higher than 95% are excluded from the linear least-squares regression, used to extract the approximate linear relationship between the two properties (i.e. zenith cloud fraction and incoming longwave radiation). Totally overcast conditions, associated with cloud fraction greater than 95%, form a different regime with respect to emitted longwave radiation, and their addition to the least-squares regression would create a bias to the result. The linear least-squares fit can be seen in the middle panel of Fig. 2.3; the correlation coefficient (~0.85) indicates that this fit accounts for approximately 72% of the variance. This linear equation is then used to approximate cloud fraction for the time periods that the ceilometer was working on reduced sensitivity (Fig. 2.3, lower panel).

The corrected cloud fraction values account for 27.5% of the total hourly cloud fraction estimates (99 and 360 respectively, over a span of 15 days – December 6-20). However, the fact that the linear fit explains 72% of the variance adds considerable uncertainty to our results. To evaluate this uncertainty, the methodology described above was applied to the EPIC and Stratus 2003 observations. The respective scatterplots, linear fits and correlation coefficients are shown in Fig. 2.4. The similar correlation coefficients between the Stratus 2003 and Stratus 2004 analysis results substantiate the use of the

Stratus 2003 observations for evaluating the accuracy of our approximation technique. Thus, hourly cloud fraction estimates were reproduced from the IR flux measurements through least-squares regression and compared with the respective zenith cloud fraction values measured from the ceilometer for the entire Stratus 2003 observational period. This comparison revealed that over 75% of the reproduced cloud fraction estimates were within 20% difference of the initial ceilometer-derived values. Further, the average cloud fraction value for the entire cruise period was not affected at all by the approximation technique. These results validate the use of the Stratus 2004 corrected cloud fraction estimates for the rest of our analysis.

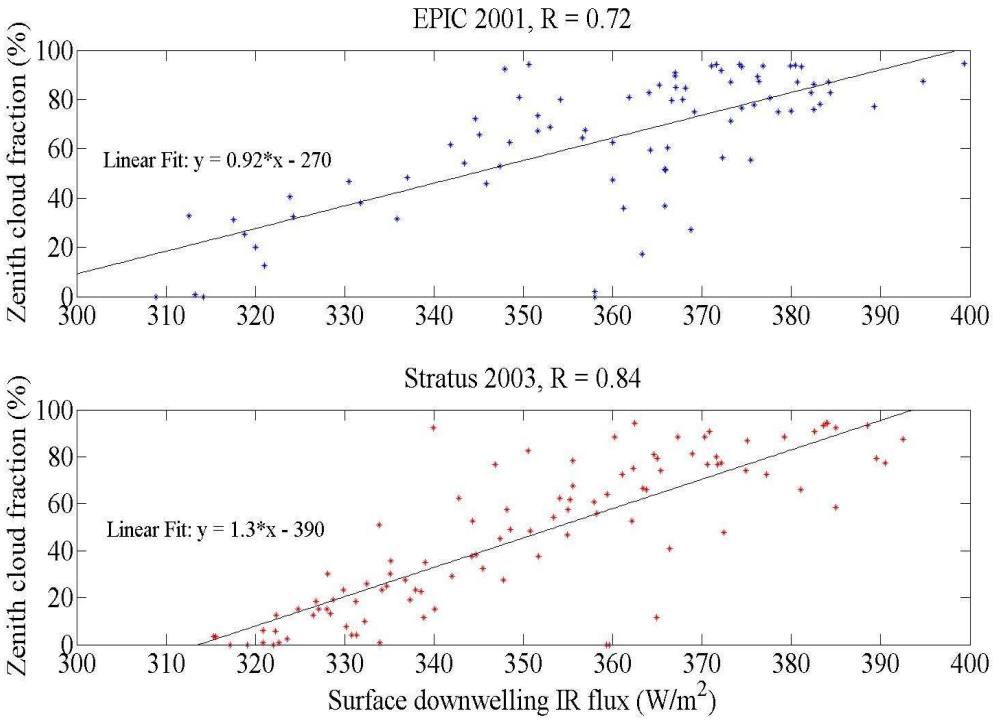

Figure 2.4: Surface longwave radiative flux as a surrogate of zenith cloud fraction for EPIC (upper panel) and Stratus 2003 (lower panel). The linear fits are plotted with straight lines, and the respective equations and correlation coefficients are also displayed. Values of cloud fraction greater than 95% have been excluded to improve the linear fits.

Chapter 3 – Boundary Layer Structures and Cloudiness

3.1 Introduction

In this chapter the temporal and spatial variability of the various boundary layer and cloud properties during each of the three research cruises and the differences between the existing three years of observations are highlighted. Directly-measured parameters as well as Value Added Products (VADs) are being considered in this section of the analysis and include: cloud base height and zenith fractional cloudiness, derived with the use of ceilometer data; cloud top height and drizzle occurrence from radar data; cloud thickness from a combination of ceilometer and radar data; potential temperature, mixing ratio, inversion strength and thickness, wind speed and direction from the soundings; radiative (incoming Solar and Infrared) and turbulent (sensible and latent heat) fluxes, SST and surface air temperature, from the instruments included in the NOAA/ETL flux suite; LWP from the microwave radiometer data.

The observed cloud and boundary layer parameters are compared among the three cruises through cruise-composite time-height profiles, which also allow for the examination of the characteristics of each cruise separately. The differences in domains associated with the latitudinal and longitudinal variability of boundary layer structure and cloudiness are also described to provide a spatial perspective to the temporal variability. The diurnal cycle of some of the key properties (e.g., fractional cloudiness, drizzle occurrence) is then examined, mainly with the use of histograms. The final section of the chapter explores the vertical layering structure of the boundary layer in the subtropical

SE Pacific stratocumulus regime; the characteristics of the inversion layer are studied and analyzed to better comprehend the moisture and heat exchange processes between the boundary layer and the free air above, and examine how these processes affect cloudiness and drizzle occurrence.

3.2 Cruise-Composite Mapping of Basic MABL Properties

3.2.1 Moisture Structure and Cloud Boundaries

During all three cruises, a wide range of cloud conditions were encountered that included extensive periods of complete cloud cover, broken-cloud and clear-sky periods. A closer look at the data reveals qualitative differences in the MABL structure and cloud conditions from year to year. A well-mixed stratocumulus-capped boundary layer was observed throughout the entire EPIC 2001 cruise (Bretherton et al. 2004). The fact that few broken-cloud and nearly no clear-sky periods were reported is confirmed by the very high cruise-averaged ceilometer derived zenith cloud fraction value (almost 92%). Conditions differed, however, during the Stratus 2003 cruise (Kollias et al. 2004). The MABL structure was occasionally characterized by the strong capping inversion and often well mixed vertical thermodynamic structure observed in 2001, but there were also days – especially at the ORS location – with moderate vertical gradients of potential temperature and mixing ratio. This was reflected in the cloud coverage, with a reduced average cloud fraction (about 82%) with respect to EPIC 2001, and the rare presence of decoupled layers with shallow cumuli clouds, which were not observed before. Although

most of the general features observed in 2003 were also present during Stratus 2004, the analysis of the data collected during the third cruise in the subtropical SE Pacific stratocumulus regime reveals further differences and interesting features with respect to the previous field experiments. The boundary layer was relatively well-mixed in the beginning of the cruise (westerly route towards the ORS location), with rather thin clouds and a good correspondence between LCL and cloud base. Conditions changed drastically, however, while the ship was stationed at the buoy location; the boundary layer started deepening significantly and strong gradients of temperature and moisture built up. These conditions persisted throughout the southeasterly course towards the South American coast and maintained a “decoupled” boundary layer for several days, that was characterized by very high and relatively thinner stratocumulus clouds and the formation of a second cloud base of cumuli clouds rising into the stratocumulus.

The MABL mixing ratio structures from the rawinsondes launched during the three cruises are shown in Fig. 3.1. The cloud boundaries and the lifting condensation level (LCL) are also displayed. The three panels of Fig. 3.1 clearly demonstrate the differences between the boundary layer and cloud structures captured during the three observational time periods and constitute a point of reference for the complexity and variability of the SE Pacific stratocumulus regime. A goal of this study is to accurately document and explain the observed variability in terms of large-scale dynamics and boundary-layer processes, and to address the issue of whether the variability is mostly driven by large-scale dynamics and atmospheric (or even oceanic) circulation or it is entirely due to internal MABL dynamics (Rozendaal and Rossow 2003).

An unexpected feature observed during Stratus 2004 is the significant height increase of the sharp inversion that capped the MABL while the *Brown* remained stationed. The inversion height was about 1.2 km at the beginning of the 2004 buoy period (same levels as EPIC 2001 and somewhat lower than Stratus 2003), but its gradual increase resulted in an all-year ORS-location high of 1.7 km about three days later – a value that remained almost constant for the remaining two days of the period. After the ship left the WORS station and headed southeast, the height of the inversion increased even more, extending to 1.8-1.9 km, before decreasing to a minimum (~500 m) near the coast (lower panel of Fig. 3.1). These larger boundary layer depths are significant given that, during EPIC 2001 and Stratus 2003, such a pronounced deepening of the boundary layer was not encountered and the maximum inversion heights observed did not exceed 1.5 km. A smaller-scale deepening of the boundary layer did take place in the beginning of these two cruises and seems to be associated with the southerly route towards the mooring location and into the stratus deck; it is worth noting that both times the inversion base height increased from about 1 km at the equatorial areas to about 1.4 km at the buoy location. During the 2001 and 2003 buoy periods, however, the boundary layer actually became somewhat shallower with the course of time. From 1.4-1.5 km upon the arrival at the ORS station in 2003, the boundary layer depth decreased gradually to about 1.1 km three days later, deepened again during the following two days by about 200 m and remained approximately constant at 1.3 km until the end of the cruise, including the easterly route to Arica (middle panel of Fig. 3.1).

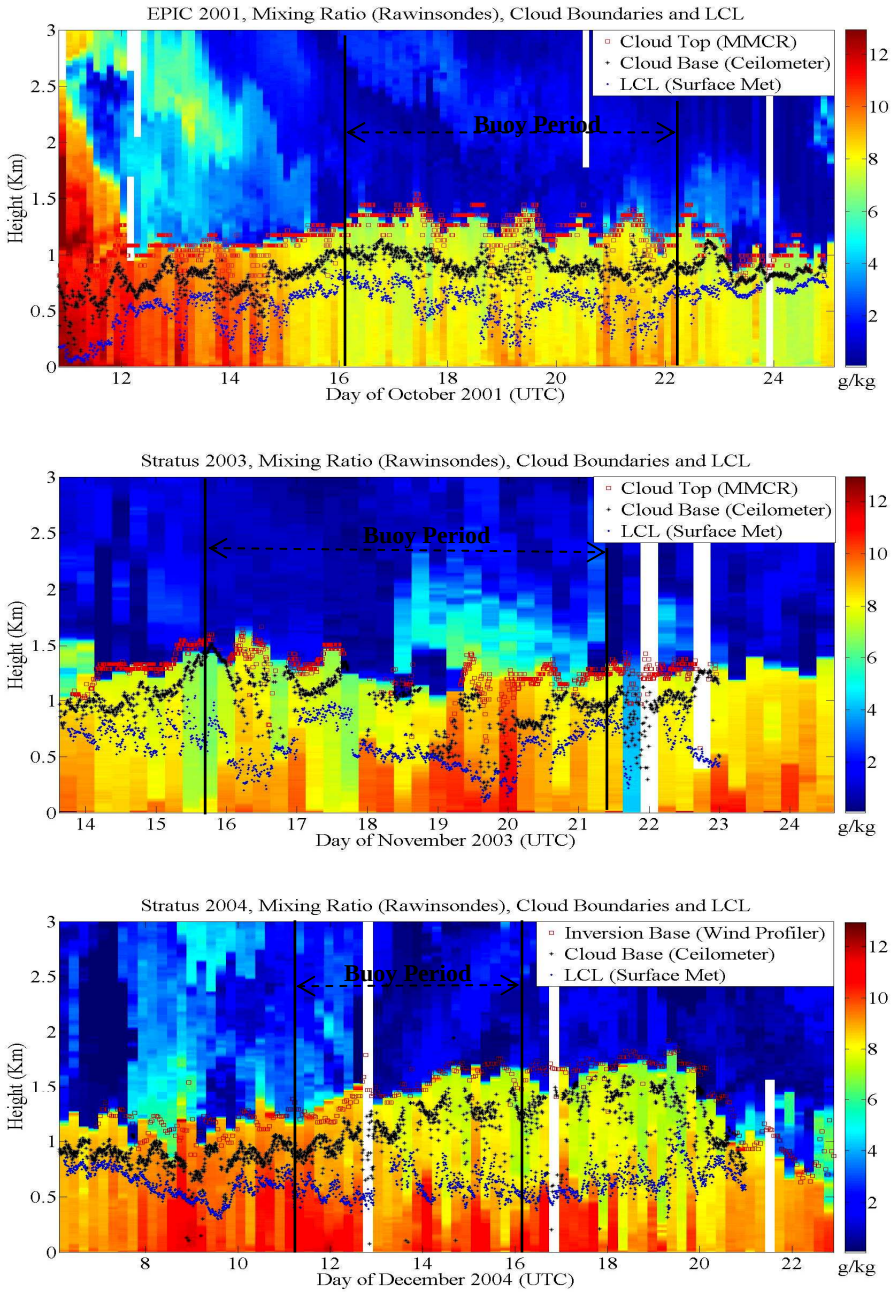

Figure 3.1: Time-height mapping of mixing ratio *r* (g/kg) from the soundings launched during EPIC 2001 (upper panel), Stratus 2003 (middle panel) and Stratus 2004 (lower panel). The cloud boundaries and the LCL are also displayed. The cloud top (red) is retrieved from the MMCR for EPIC and Stratus 2003, while for Stratus 2004, it is approximated by the inversion base height, derived from the wind-profiler reflectivity. The cloud base (black) is derived from the ceilometer and the LCL (blue) from surface met data. All estimates are 10-min averaged or linearly interpolated from a higher resolution, with the exception of the hourly averaged inversion base height. The periods when the vessels were stationed at the WHOI buoy (20°S, 85°W) are bounded by black vertical lines, while white segments indicate missing or bad sounding values.

The upper panel of Fig. 3.1 also shows that the mean daily inversion height is lowering slightly with time during the EPIC buoy period, although the dominant effect is a pronounced diurnal cycle, as described in Bretherton et al. (2004). Some signs of a similar diurnal variability in the inversion height can be seen at the moisture structure observed in 2003 and 2004 (middle and lower panels of Fig. 3.1), although the cycle is weaker and much more irregular. This could be partially attributed to the reduced frequency of rawinsondes launches during 2003 and 2004. The cloud base height does show a strong diurnal variability during Stratus 2004, in contrast to the EPIC observations that showed a pronounced diurnal cycle of inversion height/cloud top and almost no cloud base diurnal variability. Bretherton et al. (2004) point out, however, that they were expecting most of the cloud thickness variations during EPIC to come from a varying cloud base rather than inversion height variations, based on prior observations (e.g., Minnis et al. 1992) and modeling studies (e.g., Bougeault 1985). Further assessments and a mechanism for explaining the observed diurnal variability of cloud base will be explored in chapter 4. Further, some of the gaps observed in the cloud base retrievals of Stratus 2004 (especially after December 13) are mainly due to the malfunctioning of the ceilometer during the daytime, and are not necessarily associated with the non-existence of clouds (see section 2.4).

Fortunately, the ceilometer malfunction did not affect the representation of the cloud base height increase during the boundary layer deepening observed after December 13. These features also highly correlate with the onset and gradual intensification of strong vertical gradients of the boundary layer moisture and significant divergence between LCL and cloud-base height, indicating that the subcloud layer remains “decoupled” for

several days. During this time the stratus clouds are partially disconnected from the surface temperature and moisture fluxes (Bretherton and Wyant 1997; Wood and Bretherton 2004). This decoupling during the 2004 cruise appears to begin the third day that the *Brown* is stationed at the buoy location and is actually enhanced during the southeasterly route that was followed afterwards. The decoupling also seems to result in a decrease of the cloud thickness and the intermittent presence of shallow cumuli clouds below the high stratocumulus cloud base. Signs of this are indicated by the ceilometer cloud base estimates (black dots near 600-800 m in the lower panel of Fig. 3.1). The daily ceilometer backscatter intensity and cloud base height were compared with FMCW reflectivity data, revealing that some of the low-level cloud-base returns correspond to drizzle, while the rest are associated with low cumulus clouds. Examples of these plots are shown in the Appendix (Fig. A1 and A2).

Another spatial domain of interest comes from the similar easterly route that the *Brown* and the *Revelle* followed after leaving the WHOI buoy during EPIC and Stratus 2003 respectively. This transect along the 20°S parallel from the ORS location (85°W) to Arica, Chile (~70°W) is repeated in Stratus 2004 (hereafter the 20°S transect), but in the opposite direction, since Arica was then the departure – and not the ending – point for the *Brown* (unlike EPIC and Stratus 2003 that were initiated in equatorial areas – see Fig. 2.1). During the EPIC transect, the boundary layer becomes somewhat shallower. More specifically, one day after the departure from the buoy, the inversion height dropped to the lowest value of the entire period of observations (~850 m at 80°W), but then slightly increased again and remained around 1 km for the remaining two days of the cruise. During this period, the boundary layer was even more well-mixed than the southerly

transect and the buoy period, the LCL and cloud base were more coherent and matched even better than before, but the clouds were thinner due to the lower inversion heights. The respective transect in Stratus 2003 was characterized by a constant inversion base height of approximately 1.3 km, as we mentioned earlier, and an interchange between weak and moderate vertical gradients of temperature and moisture, similar to the previous days of the cruise. The mixing ratio values recorded during the Stratus 2003 transect are much higher (~ 8-10 g/kg) than the respective 2001 period (~ 6-8 g/kg). The same applies for the 2004 transect (beginning of Stratus 2004); the boundary layer remains well-mixed throughout, but with very high moisture content (~ 9-12 g/kg). After a gradual decrease during the first two days of the cruise, the inversion base rises again to reach 1.2 km at the beginning of the buoy period.

Another notable feature in Fig. 3.1 is the high moisture content above the inversion observed at certain time periods in all three cruises. In order to get a better view of the upper level moisture, the relative humidity (RH) profiles up to 10 km are shown in Fig. 3.2. Layers of dry and moist air can be seen descending with time during all three cruises. This feature, which seems to be more pronounced in 2001 and 2004, may be attributed to the persistent subsidence over this region (Bretherton et al. 2004). The area of the SE Pacific that the cruises were held is part of the descending branch of the local Hadley Cell; this is consistent with relatively high mean downward vertical motion (subsidence) in the mid- and lower troposphere, and possibly the descent of layers with high moisture content, originating from the deep convection that takes place over the Intertropical Convergence Zone (ITCZ). Another possible source of the upper-level moisture could be the deep convection forming over the Amazon and the surrounding areas of South

America, rising high above the Andes and being transferred over the SE Pacific area through westward-propagating upper- or mid-tropospheric Rossby waves (Bretherton et al. 2004). A sign of this circulation pattern could be the unexpected high moisture content of the upper-level air masses located close to the South American coast, as indicated in Fig. 3.2 from the high relative humidity values between 4 and 10 km during the 20°S transect in all three cruises.

The moist air above the MABL during the initial days of the EPIC cruise is possibly a manifestation of the deep convection over the equatorial areas (the EPIC cruise was initiated at the Galapagos Islands and the first sounding shown in the upper panels of Fig. 3.1 and 3.2 was released approximately at 2°S, 95°W). Unfortunately, the middle panels of Fig. 3.1 and 3.2 are not suitable for evaluating the existence of equatorial deep convection – if any – during Stratus 2003, since the first sounding in the cruise was launched when the *Revelle* had already reached 10°S, 85°W.

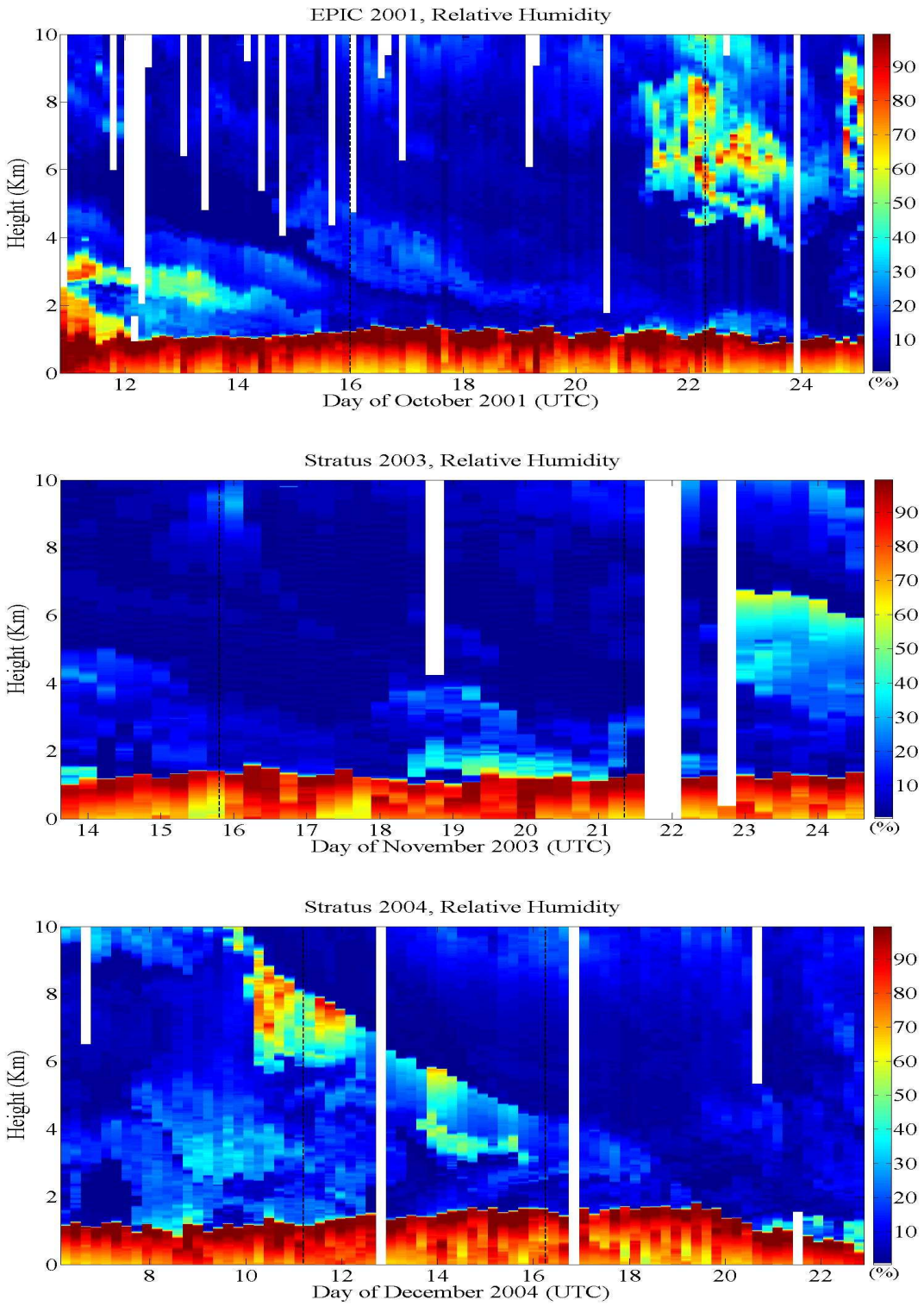

Figure 3.2: Time-height mapping of relative humidity RH (%) from the soundings launched during EPIC 2001 (upper panel), Stratus 2003 (middle panel) and Stratus 2004 (lower panel). Dashed lines indicate the period when the ship was stationed at the WHOI buoy; white segments indicate missing or bad sounding values.

3.2.2 Air Temperature Profiles and SST

The evolution of potential temperature during the three research cruises – for the lower 2 km of the troposphere – is illustrated in Fig. 3.3. As expected, the potential temperature structure for all three cruises is characterized by the strong capping inversion that was presented and described before with the use of the respective mixing ratio plots. The boundary layer temperature during EPIC demonstrates an almost uniform profile after the *Brown* moved away from the equator, although some deviations corresponding to colder surface temperatures can be seen throughout the cruise. The more pronounced of these cold-air periods takes place on the early morning (0200 local time) of October 19, and is accompanied by a very high moisture content for the entire boundary layer (relative humidity is 100% from 300 to 1300 m – see Fig. 3.4). The EPIC boundary layer temperature structure is not encountered during Stratus 2003 and Stratus 2004 that were characterized by stronger vertical potential temperature gradients. This characterization is in good agreement with the three moisture structures described in the previous section, and is yet another indication of the close interaction between temperature and moisture fluxes within stratocumulus-capped boundary layers. The EPIC boundary layer is generally colder compared with the 2003 and 2004 field experiments; potential temperature had a cruise average of 290.2 K (~17°C) for the lowest 1 km of the atmosphere, while this value was higher for Stratus 2003 (290.9 K – 17.8°C) and Stratus 2004 (291.7 K – 18.5°C). This is in response to an almost equivalent variation in SST during the respective periods (mean SSTs for EPIC, Stratus 2003 and Stratus 2004

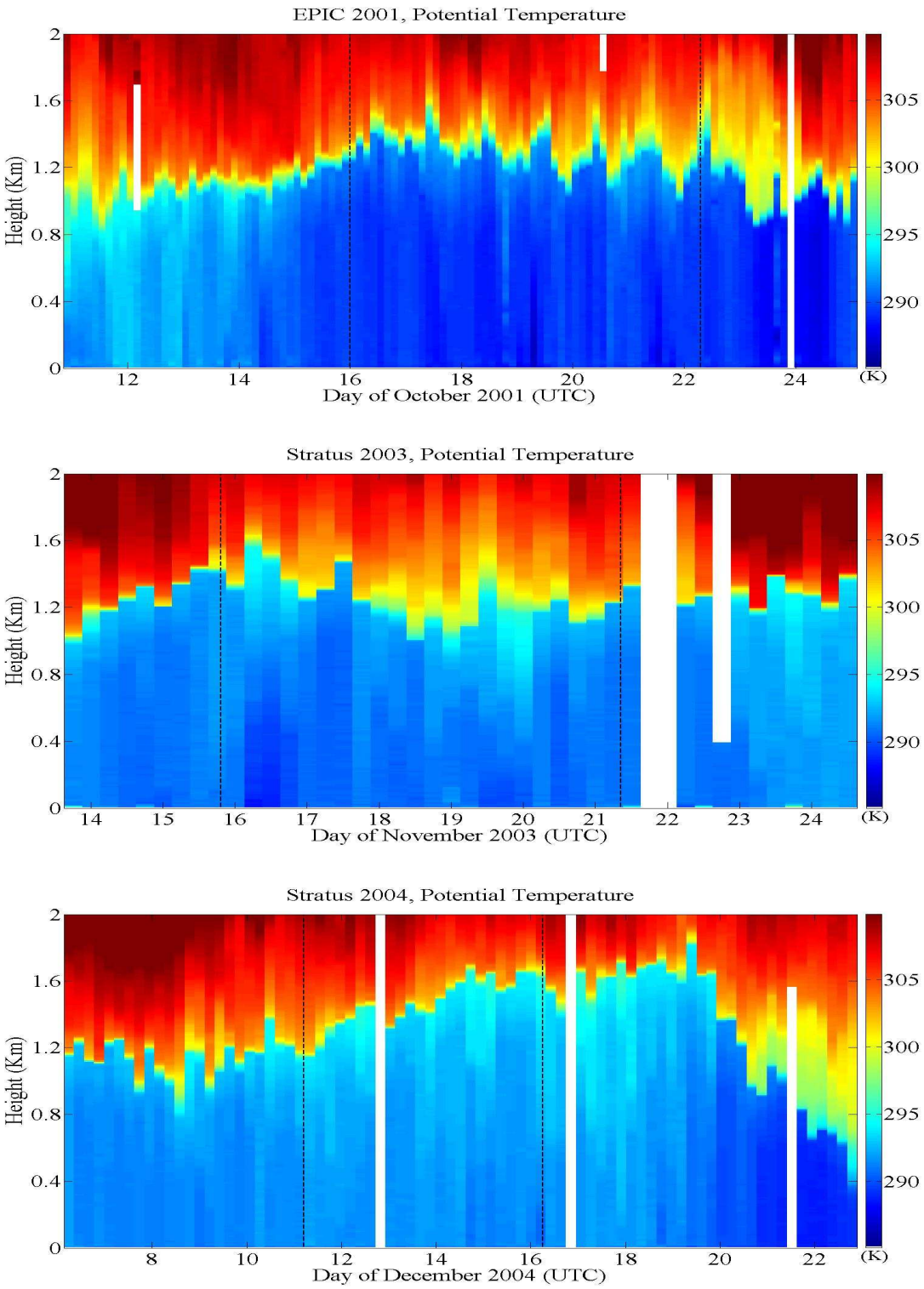

Figure 3.3: Time-height mapping of potential temperature θ (K) from the soundings launched during EPIC 2001 (upper panel), Stratus 2003 (middle panel) and Stratus 2004 (lower panel). Dashed lines indicate the period when the ship was stationed at the WHOI buoy; white segments indicate missing or bad sounding values.

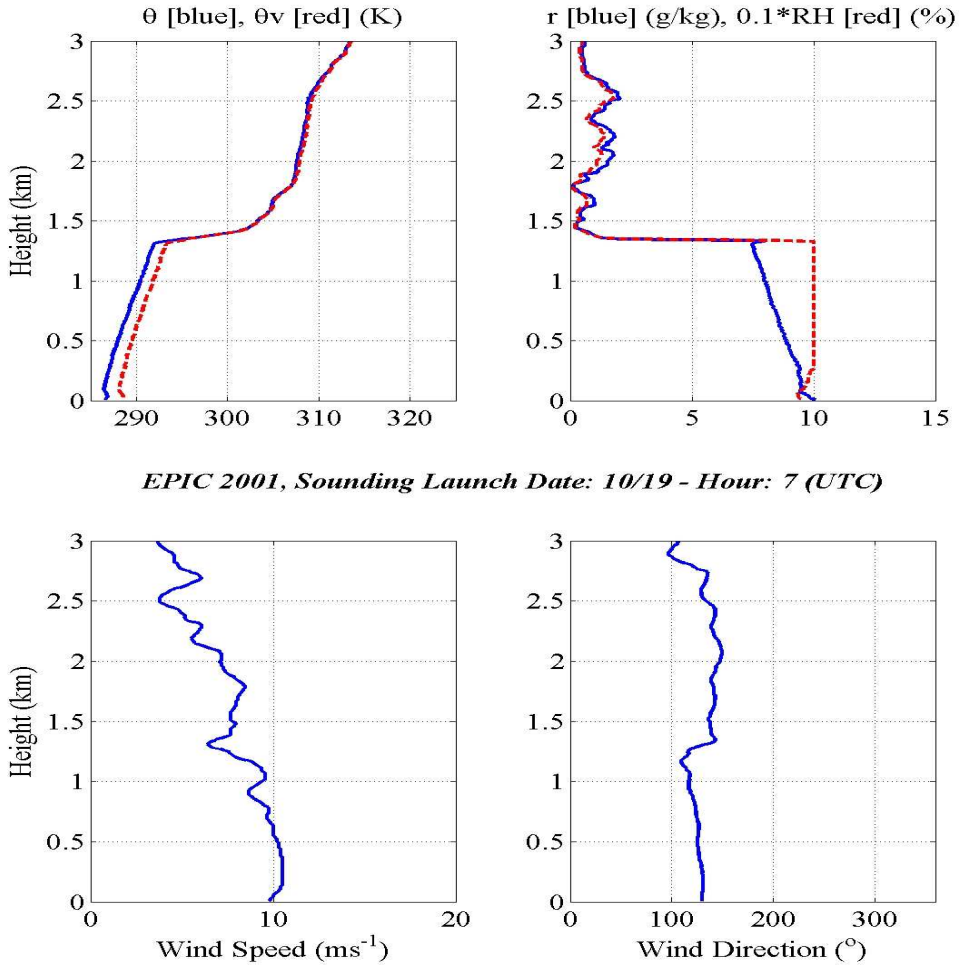

Figure 3.4: Characteristic sounding from the EPIC cruise, released on October 19, 2001 while the *Brown* was stationed at the ORS location.

were 19, 19.9 and 19.4°C respectively; the lower value for the 2004 SST cruise average can be attributed to the spatial domain of the cruise, which was further south relative to the previous field experiments), as well as in accordance with the monthly climatology (the cruises were held in successive months – October for EPIC 2001, November for Stratus 2003 and December for Stratus 2004, – covering the period from austral mid-spring to early summer).

The cruise track SSTs shown in the three panels of Fig. 3.5 for the three cruises respectively, seem to be consistent with the temporal and spatial climatology of the area. The low SSTs (~18°C) recorded on October 10 (2001) just after the *Brown* left the Galapagos Islands to reach 95°W are associated with the so-called "cold tongue" (Pyatt et al. 2005) – conspicuously cool waters about 1000 km wide, extending westward from the South American coast along the equator into the central Pacific. After the *Brown* started moving south along the 95°W line and exited the area of the cold tongue, the SST demonstrated a sharp increase of about 4°C in two days (22°C at 8°S, 95°W on October 12) and then gradually dropped again during the southeastward route that ended at the WHOI buoy location (~19°C at 20°S, 85°W on October 16). This route was also characterized by a gradual increase of the sea-air temperature difference as a result of the surface air temperature (T_{air} hereafter) dropping at a faster rate compared with the SST; the sensors onboard the *Brown* recorded almost the same values for SST and T_{air} on October 12, compared to the sea-air differences of about 2°C observed four days later at the beginning of the WHOI buoy period (Fig. 3.5, upper panel). This rapid change is probably due to the stronger cold-air advection that characterizes the core of the stratocumulus regime around the WHOI buoy location, compared with the advection rates observed in the areas south to the equator around 95°W (trade-cumulus regime). The large sea-air temperature difference was maintained throughout the EPIC buoy period, ranging approximately from 1-3°C and being primarily modulated by fluctuations of T_{air}, while SST varied slightly between 18.5 and 19°C. Very low values of T_{air} (~15°C) were recorded on two specific events: the first took place from 1400 UTC on October 18 to 1400 UTC on October 19 and the second from 0800 to 2200 UTC on October 21. Both

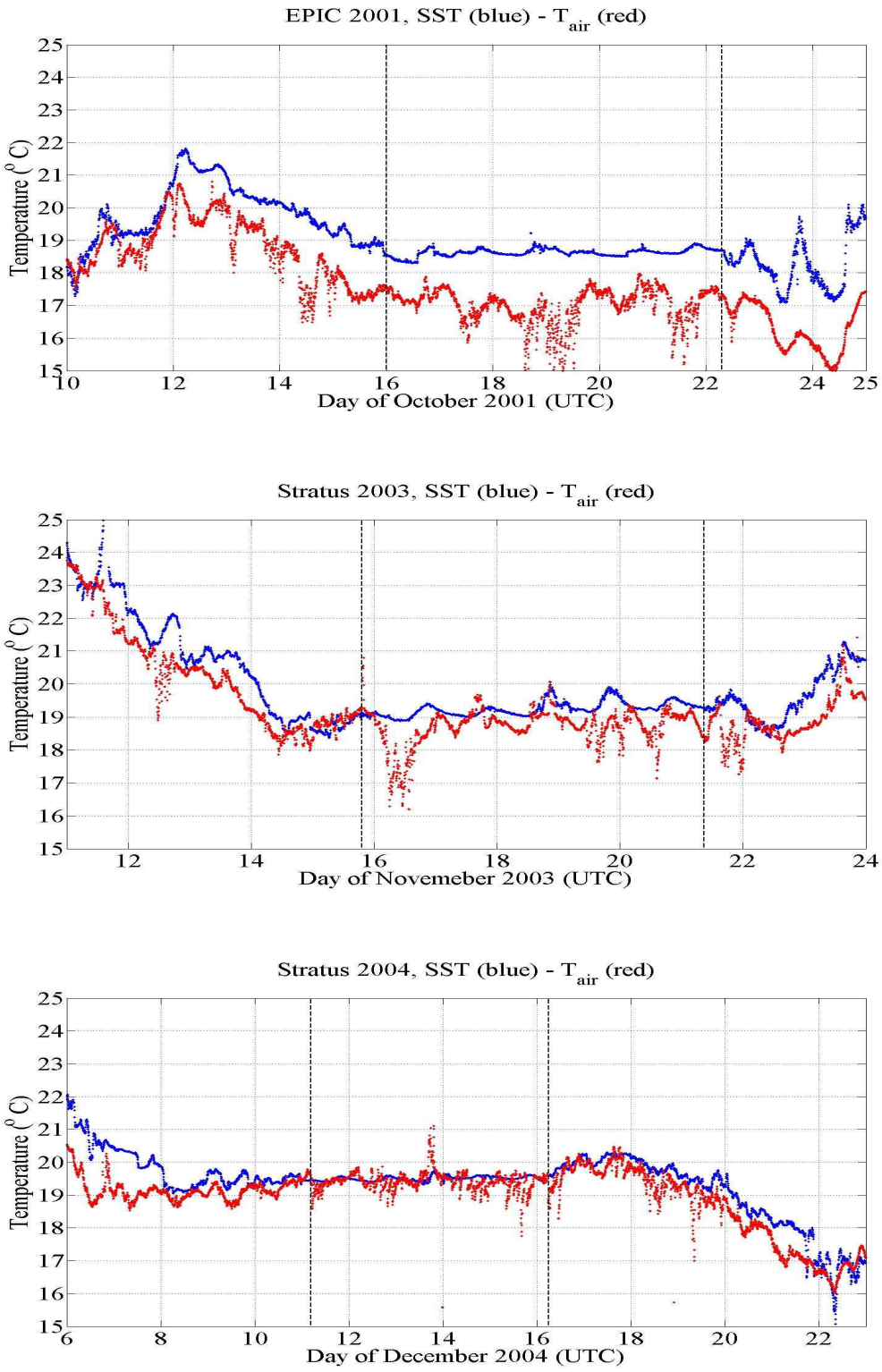

Figure 3.5: Evolution of SST (blue) and Surface Air Temperature T_{air} (red) during EPIC (upper panel), Stratus 2003 (middle panel) and Stratus 2004 (lower panel), as recorded from the NOAA/ ETL air-sea flux system. Dashed lines indicate the period when the ship was stationed at the WHOI buoy.

events induced very high values of sea-air temperature difference (~4°C), and seem to be associated with moistening and cooling of the lower 500 m of the boundary layer (see upper panels of Fig. 3.1 and 3.2 respectively), a significant decrease in LCL and its partial decoupling from the stratocumulus cloud base (upper panel of Fig. 3.1).

Although the sea-air measurements, collected for the respective domains of the 2003 and 2004 field experiments demonstrated a relatively similar variation with track to that observed during EPIC, some differences were noted. The southward route marking the initial days of Stratus 2003 is accompanied by a gradual drop in SST, equivalent to the one associated with the EPIC period of October 12-16; however, the initial SST and T_{air} values recorded in Stratus 2003 were close to 24°C, thus much higher than the respective values at the departure of the *Brown* from the Galapagos Islands in 2001. Although the latitude was the same, the absence of a pronounced manifestation of the cold tongue in 2003 seems to be associated with longitudinal differences. SST and Tair decreased rapidly as the *Revelle* steamed away from the warm equatorial waters to enter the cool stratus region of the subtropical SE Pacific, with their difference remaining at quite low levels (0-1°C) compared with the sea-air temperature difference recorded during the respective EPIC route. The SSTs during the Stratus 2003 WHOI buoy period varied between 19 and 20°C, and showed enhanced diurnal variability compared with the respective periods in 2001 and 2004. This should be attributed to the broken-cloud or clear-sky periods observed at the buoy location in 2003, especially just after the solar flux maximum (Kollias et al. 2004). Events like those during the EPIC buoy period associated with low values of T_{air} that result in a large sea-air temperature difference were observed during the 2003 buoy period as well (November 16, 19 and 20), and correlated well with

higher values of temperature and relative humidity in the lower boundary layer. The sea-air temperature difference was on average much smaller (0-1°C) than during EPIC.

The 2004 buoy period was characterized by an approximately constant SST (~19.5°C), and surface air temperatures very close to this value and at times slightly larger than that. One event of a sudden rise of T_{air} at the end of December 13 resulted in the minimum sea-air temperature difference observed on all cruises (-1.5°C) and should be further investigated. An expected decrease in SST and T_{air} – with their difference rising gradually – marked the southeastward and eastward routes of Stratus 2004, while the path along the Chilean coast that concluded the cruise was characterized by even lower SSTs but higher surface air temperatures – indicative of the coastal upwelling and the land effects influencing the ocean and boundary layer temperatures. Moreover, the 20°S transect, common with all three cruises, seems to be dominated by increasing SST and T_{air} as we move eastward closer to the coast. This is evident both on the ending part of Stratus 2003 (November 22-24, 2003) and the initial part of Stratus 2004 (December 6-8, 2004), while the concluding days of EPIC (October 22-25, 2001) are characterized by an extremely pronounced SST and T_{air} variability and cannot fully support the pattern observed in the two later cruises.

3.2.3 Wind Speed and Direction

The structure of the zonal and meridional winds from the radiosondes launched during the three field experiments are shown in Figs. 3.6 and 3.7 respectively. In all three cruises the winds are consistent with climatology, with quite strong southeasterlies

prevailing in the lower 3 km of the troposphere. Some features, however, shown in Figs. 3.6 and 3.7 indicate variability of note. First, the EPIC and Stratus 2003 pre- and post-buoy periods are accompanied by episodes of weak northwesterlies above the inversion. The EPIC episodes occurred during the periods October 14-16 (the *Brown* traveled southeastward from about 15°S, 90°W to 20°S, 85°W) and October 22-25 (the *Brown* moved eastward along the 20°S transect), and were quite pronounced with northwesterly winds persisting at levels higher than about 1 km throughout the entire periods, as seen in the upper panels of Figs. 3.6 and 3.7. The EPIC wind structure at heights above 3 km (graphs not shown here) reveals that these events are sporadic subsiding extensions of a persistent northwesterly flow aloft (above 4 km) down to the altitude of the inversion layer. Similar mesoscale variability accounts for the less pronounced event of November 15-16 (the *Revelle* was moving along the 85°W line from 15 to 20°S), that was shorter in duration and extended down to the 2-km level only. In contrast, the episode of weak westerly winds observed during November 23-25 (20°S transect) is independent of the upper-level flow and seems to be related with land-induced synoptic variability.

Another feature observed in the upper and middle panels of Fig. 3.7 is the weak northerly flow characterizing the layer between 1 and 2 km right after the beginning of the two cruises: the EPIC event occurs on October 11 during the southward route of the *Brown* (from 2 to 8°S along 95°W), and the Stratus 2003 event on November 13 when the *Revelle* was located at about 10-11°S, 85°W. The flow on November 13 is further characterized by a weak westerly wind component, as observed in Fig. 3.6. These events are suggestive of the so-called shallow meridional circulation; southerly trades in the

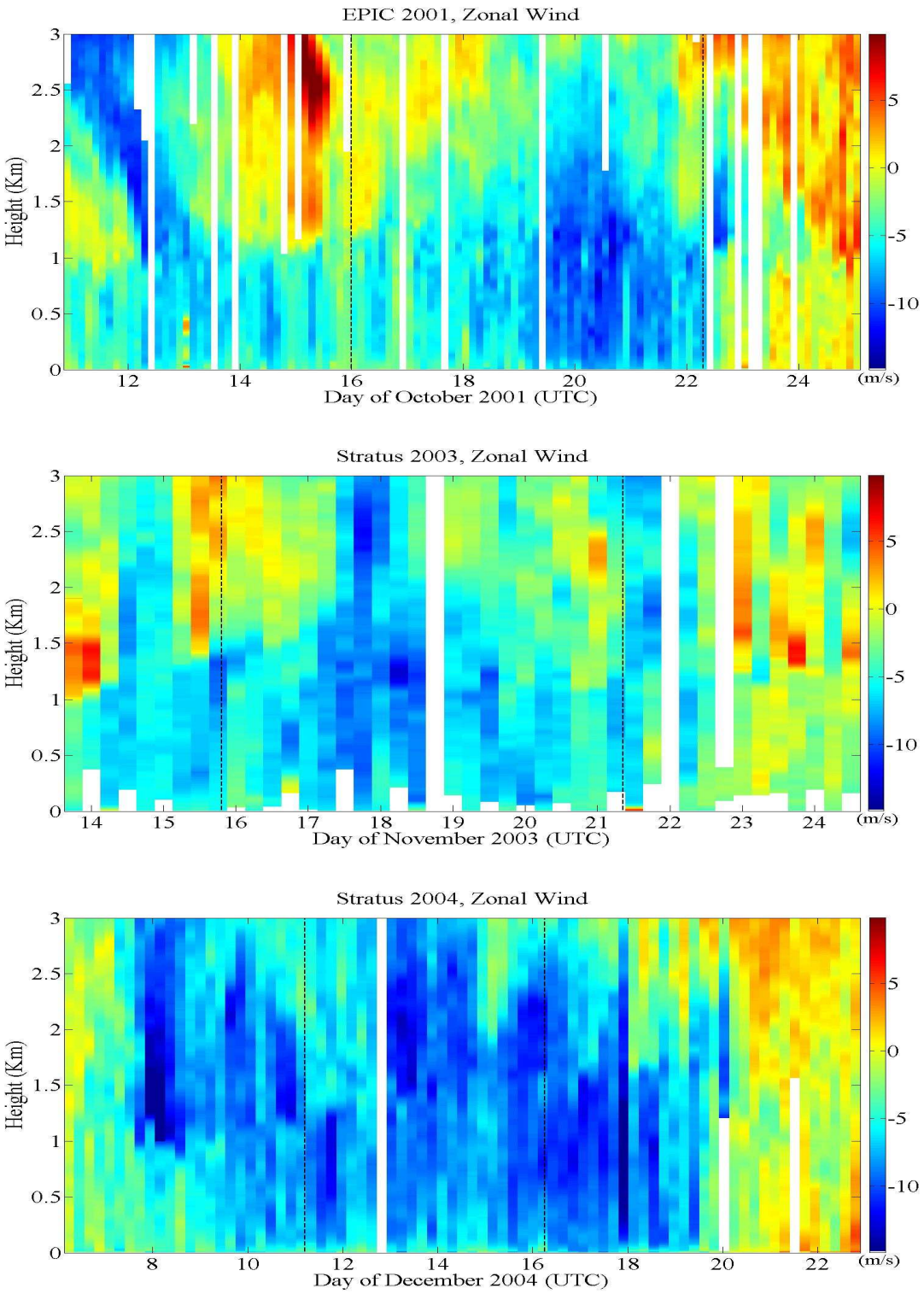

Figure 3.6: Time-height mapping of zonal wind speed from the soundings launched during EPIC 2001 (upper panel), Stratus 2003 (middle panel) and Stratus 2004 (lower panel). Positive winds are to the East. Dashed lines indicate the period when the ship was stationed at the WHOI buoy; white segments indicate missing or bad sounding values.

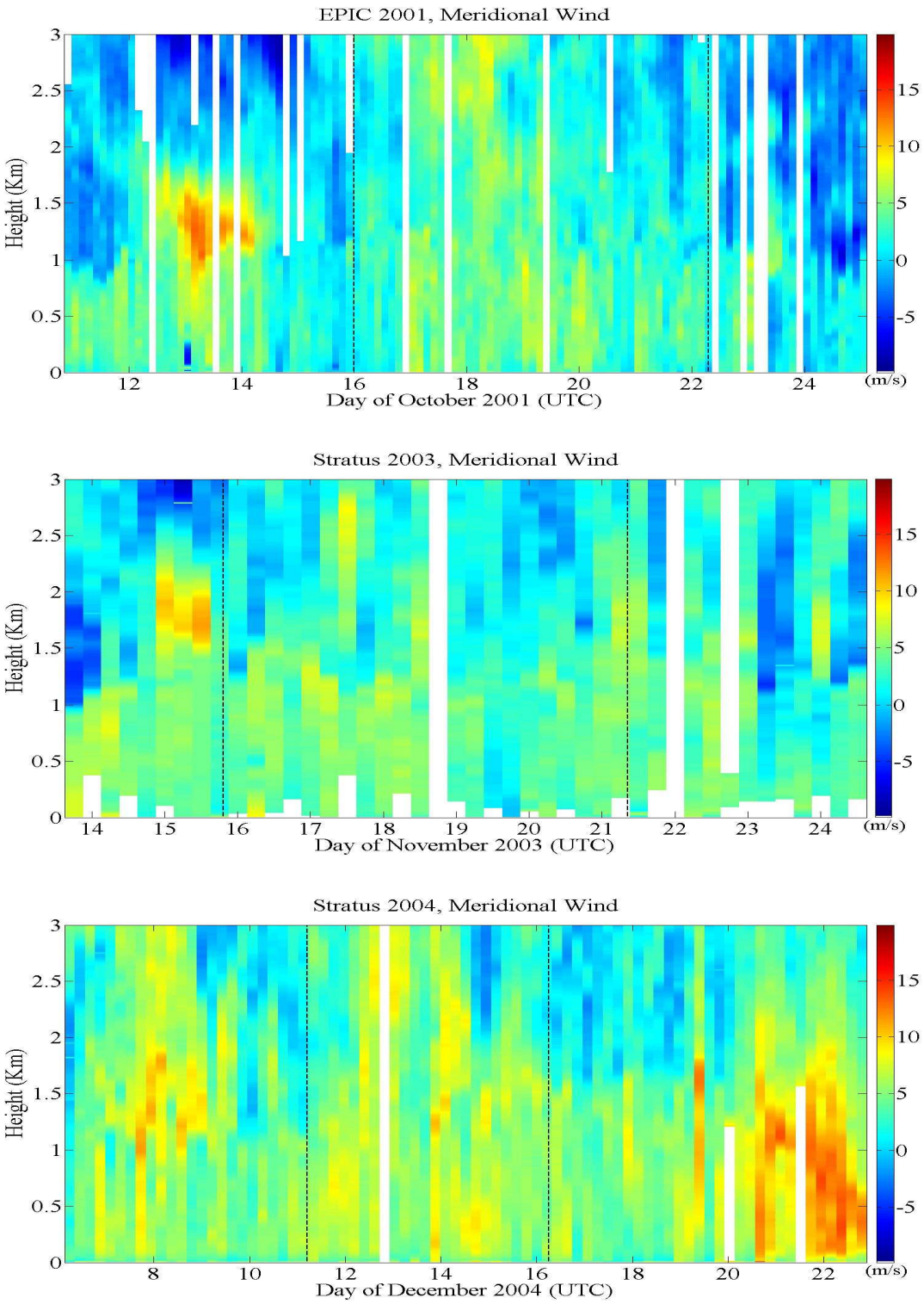

Figure 3.7: As in Fig. 3.6, but for the meridional wind speed. Positive winds are to the North.

MABL and a low-level return flow from the ITCZ atop the MABL (Zhang et al. 2004). Provided that the Stratus 2003 event is indeed associated with the shallow meridional circulation cell and is not linked to some kind of synoptic perturbation, it may very well constitute the southern- and easternmost record of this northerly low-level return flow, since all previous observational evidence of this flow was found in a domain of the eastern tropical Pacific bounded to the south and to the east by the 8°S and 95°W lines respectively. This assessment ambiguity notwithstanding, both events imply enhanced moisture advection – at the height of the MABL top – from the ITCZ into the northern edge of the subtropical southeast Pacific stratocumulus regime, and could influence low-level cloudiness in the area (Zhang et al. 2004). As a matter of fact, increased moisture content can be seen right above the boundary layer during both time periods (October 11, 2001 and November 13, 2003) that the low-level northerly flow was observed (see Figs. 3.1 and 3.2). Thus, it would be interesting to clarify the source of the specific observation, especially for the EPIC period that is associated with very high values of mixing ratio/relative humidity above the MABL: is it advection of ITCZ-originated moist air due to the upper branch of the shallow meridional circulation, or deep convection over the areas south of the equator, as we mentioned earlier in section 3.2.1?

The profile of wind direction in the lower 3 km of the atmosphere during Stratus 2004 was the most invariant among the three cruises; strong southeasterlies were predominant in the MABL from the beginning of the cruise till the point that the *Brown* reached 26°S, 80°W on December 20, while above the inversion the southeasterly flow interchanged at times with winds originating from the east or the northeast (December 9-11, December 16-20). This trend of winds blowing more from the east (rather than the southeast) above

the MABL was occasionally observed during EPIC and Stratus 2003 as well, as seen in the upper and middle panels of Figs. 3.6 and 3.7. A notable feature in the 2004 field experiment is the southerly/southwesterly flow that characterized the MABL during the eastward route towards- and the southward route along the Chilean coast (December 20-23). This flow is likely to be a manifestation of the low-level jet off the west coast of subtropical South America; the existence of this jet has been suggested by several observations in the past (e.g., Rutllant 1993), but its structure and dynamics were just recently addressed by Garreaud and Munoz (2005) using Quick Scatterometer (QuickSCAT) surface wind data. According to the later study, this jet is characterized by an elongated area of maximum wind speed (~8-10 m/sec) off central Chile, which has a cross-shore width of about 500 km (76°-72°W) and reaches a maximum extent and most poleward position (29°-37°S) from November to February. The analysis of the three-dimensional structure of a well-defined event in October 2000 using observed and model-derived vertical wind profiles revealed that the jet core resides at the MABL top and actually slopes towards the coast as the boundary layer gets shallower. The Stratus 2004 dataset seems to provide further evidence to the previous assessments; the apparent southerly jet event during December 21-23, when the *Brown* traveled from about 26° to 32°S along the 72°/73°W lines, is very pronounced with maximum winds (12-14 m/sec) occurring indeed at or slightly above and below the height of MABL top. In addition to the evaluation of the low-level jet spatial and temporal distribution, Garreaud and Munoz (2005) found a correlation between the jet events and increased cloudiness in the region downstream of the maximum winds along the coast and farther offshore, as well as an interconnection of such events with the strengthening of the subtropical anticyclone over

the SE Pacific. These findings could play a crucial role in the understanding and interpretation of the observed Stratus 2004 boundary layer structure and cloudiness, since the respective cruise period is associated with positive anomalies of the SE Pacific anticyclonic circulation, as well as with enhanced cloudiness in the proximity of the WHOI buoy location despite the existence of persistent decoupling.

Figs. 3.6 and 3.7 also reveal a distinct difference among the three cruises regarding the strength of the southeasterlies that prevailed in the lower troposphere. The sharp pressure gradients, forming as a result of the enhanced anticyclonic circulation over SE Pacific during Stratus 2004 (graphs not shown here), seem to be primarily responsible for the strong trade winds observed in and above the MABL throughout the cruise. From December 10 to December 20, zonal and meridional winds were constantly higher than 8-9 and 5-6 m/sec respectively, and similar values were observed above the MABL during the 20°S transect and the WHOI buoy period (December 7-11 and December 12-16 respectively). Such high wind speeds were not observed during the previous field experiments. There were, however, a few – relatively short – time periods through the duration of EPIC and Stratus 2003 that indicated a jet-like structure associated with strong zonal or meridional winds: October 12-14 (2001), while the *Brown* was traveling southeastward from 8°S, 95°W to about 15°S, 90°W with high meridional winds at and above the MABL top, and October 19-22 (2001) and November 17-19 (2003), while at the buoy location with strong zonal winds covering the entire extent of the boundary layer. Another notable feature is that winds in EPIC and Stratus 2003 are stronger in the MABL than above, although the temperature and moisture inversion does not directly reflect to the wind structure in any of the cruises.

3.2.4 Radiative and Turbulent Fluxes

Surface radiative and turbulent fluxes are among the processes that greatly influence the vertical structure of stratocumulus-capped boundary layers and are coupled to the cloud cover and lifecycle. Time series of surface incoming solar and IR fluxes measured continuously from the NOAA/ETL air-sea flux system during the three cruises are displayed in Fig. 3.8 and the respective records for surface latent heat (LH), sensible heat (SH) and virtual heat (VH) fluxes are shown in Fig. 3.9.

Both incoming shortwave and longwave radiation demonstrate a rather expected variability throughout each cruise, as they are primarily modulated by fractional cloudiness. During periods with overcast skies, the IR flux ranges from 390 to 410 W/m^2 while the maximum (noontime) solar flux varies between 600 and 800 W/m^2. As expected, clear-sky periods are associated with reduced incoming longwave radiation (310-320 W/m^2) and much higher noontime solar fluxes (1100-1200 W/m^2). Values in between correspond to broken-sky periods. This span of values for both longwave and shortwave radiation provides a rough estimate of the intensity of the radiative forcing associated with the SE Pacific stratocumulus cloud deck, and highlights the importance of an accurate representation of these clouds in the radiative transfer schemes of regional and global climate models.

The EPIC and Stratus 2003 events associated with increased drizzle occurrence and sea-air temperature difference, moistening and cooling of the lower levels of the boundary layer, and partial decoupling between LCL and cloud base (see section 3.2.2), correspond to relatively low values of incoming IR flux as well as increased shortwave

radiation that is indicative of a possible reduction in cloud cover. This will be further assessed in the following section.

The surface turbulent fluxes are primarily modulated by the sea-air temperature difference variations and the winds. The SH flux is tied to the SST-T_{air} evolution, thus is characterized by relatively high values during the EPIC cruise and significantly lower values during Stratus 2003 and 2004. Actually, intermittent periods in the later cruises are associated with negative values of SH flux. LH fluxes exhibit much higher values (in W/m^2) than SH fluxes in general, although their contribution to the VH flux (or buoyancy flux) is limited. Fig. 3.9 clearly shows that the VH flux closely follows the SH flux evolution. There is a pronounced diurnal cycle observed in the LH flux evolution during the first half of EPIC 2001, which should be further investigated. LH fluxes exhibit large variability in Stratus 2003, especially during the WHOI buoy period, in contrast to Stratus 2004, when the LH flux values range between 50 and 150 W/m^2 throughout the cruise.

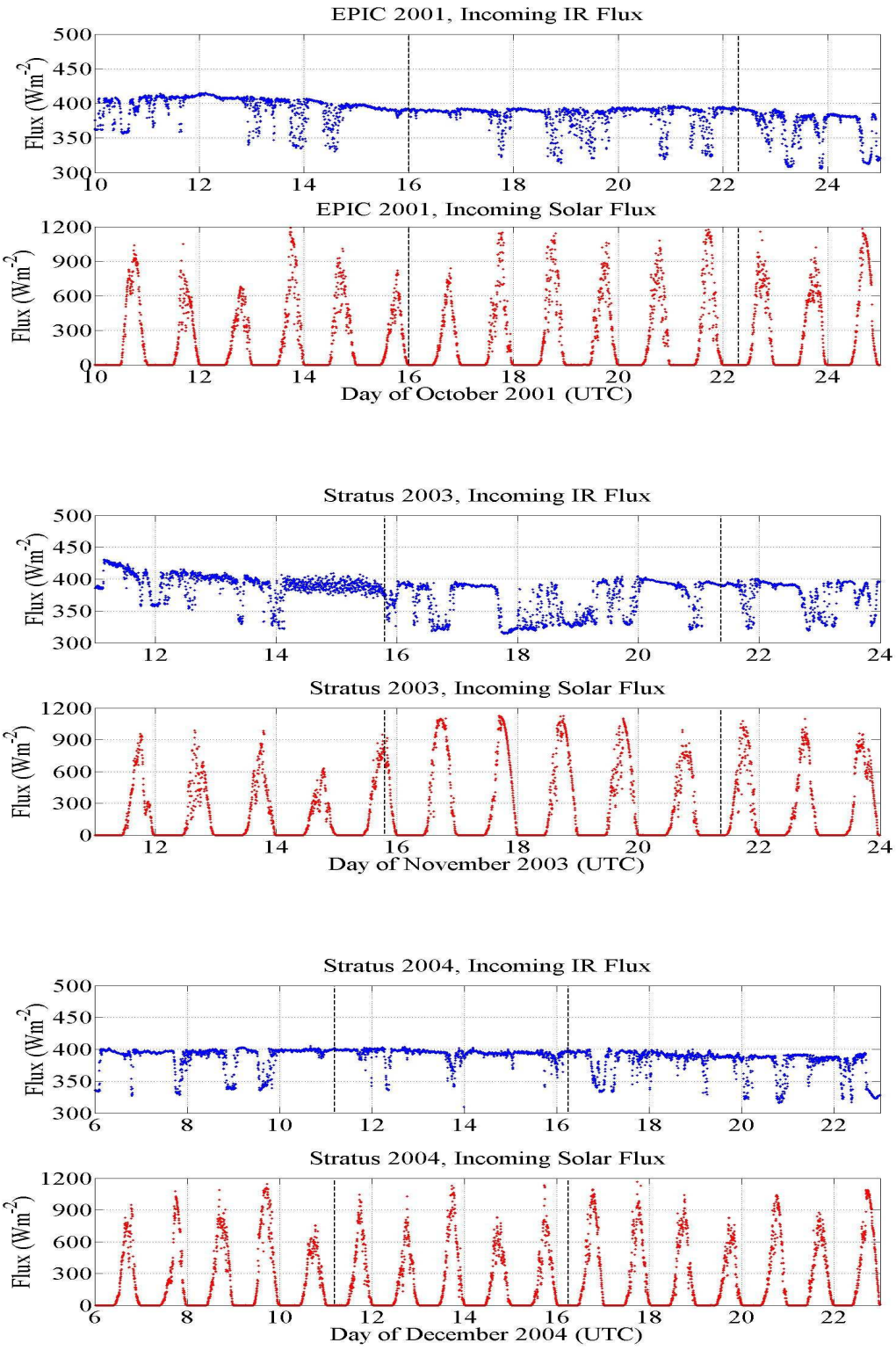

Figure 3.8: Incoming longwave (blue) and shortwave (red) radiation during EPIC (upper panel), Stratus 2003 (middle panel) and Stratus 2004 (lower panel). Dashed lines indicate the period when the ship was stationed at the WHOI buoy.

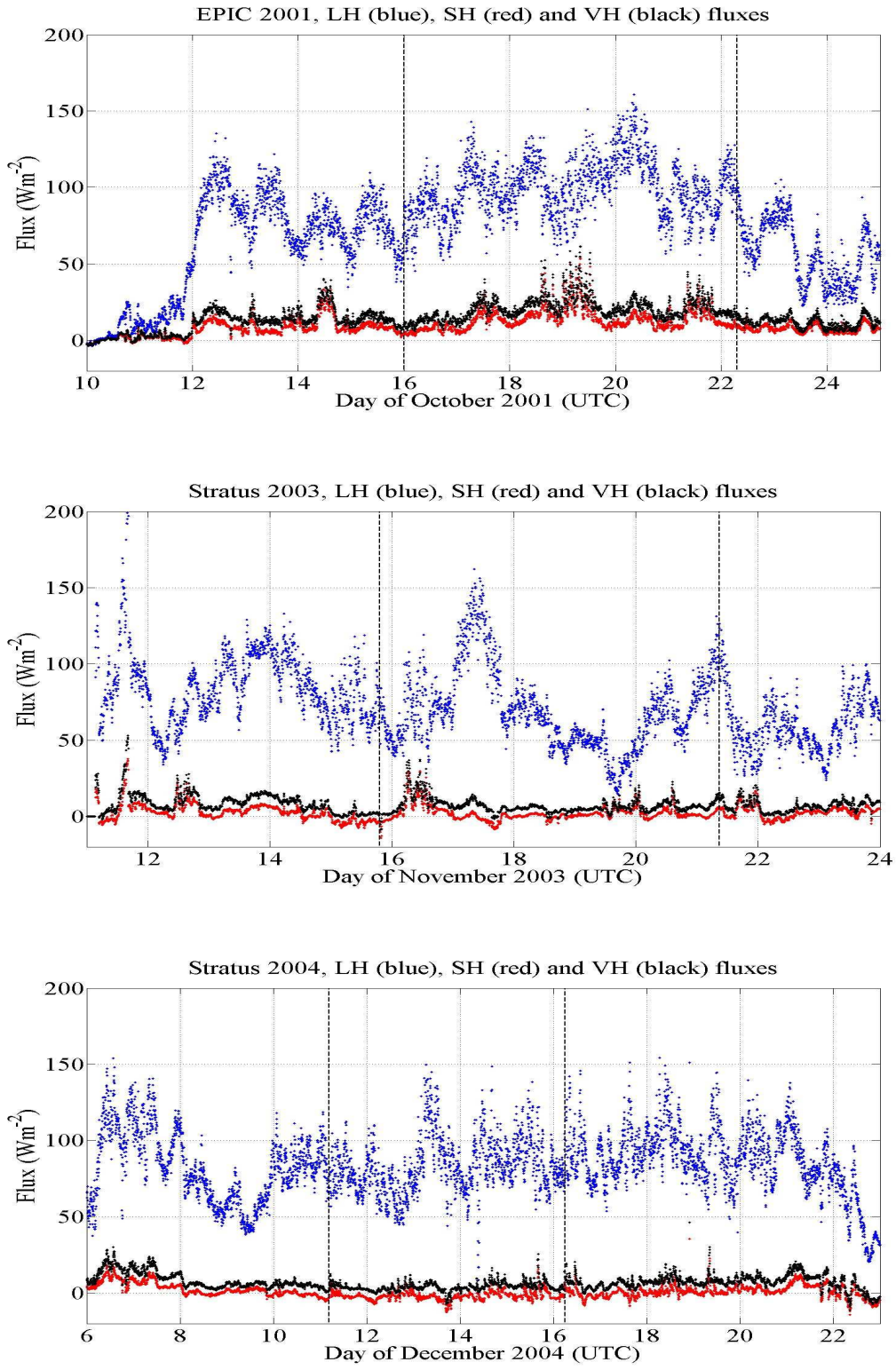

Figure 3.9: Surface latent heat (blue), sensible heat (red) and virtual heat (black) fluxes during EPIC (upper panel), Stratus 2003 (middle panel) and Stratus 2004 (lower panel). Dashed lines indicate the period when the ship was stationed at the WHOI buoy.

3.2.5 Fractional Cloudiness, Drizzle Occurrence and LWP

The investigation of the relationship between fractional cloudiness, drizzle occurrence and LWP requires detailed analysis of measurements from the ship-based active and passive sensors. Millimeter wavelength Doppler radars have high temporal and spatial resolution, extreme sensitivity and high velocity resolution. Due to their short wavelength, millimeter radars are capable of detecting very small droplets with diameters of 5-10 microns. Furthermore, millimeter radars have narrow beams that result in small sampling volumes. As a result, these radars provide excellent resolution in space and in time (e.g., Clothiaux et al. 1995; Kollias et al. 2000). The ceilometer backscatter can be used to estimate the height of the cloud base with a temporal and spatial resolution of 15-30 s and 15 m respectively. Combined observations from the MMCR (35-GHz, NOAA/ETL) and the ceilometer are used for the retrieval of cloud boundaries and morphology in this study.

Fig. 3.10 shows the time-height mapping of MMCR reflectivity during the EPIC 2001 and Stratus 2003 cruises. As we mentioned earlier (section 2.4), there are almost no available radar data from the NOAA/ETL MMCR for the Stratus 2004 cruise. Complimentary observations from the UMRMG 94-GHz FMCW radar along with ceilometer observations are used to extract information on the cloud fraction and drizzle occurrence during this cruise.

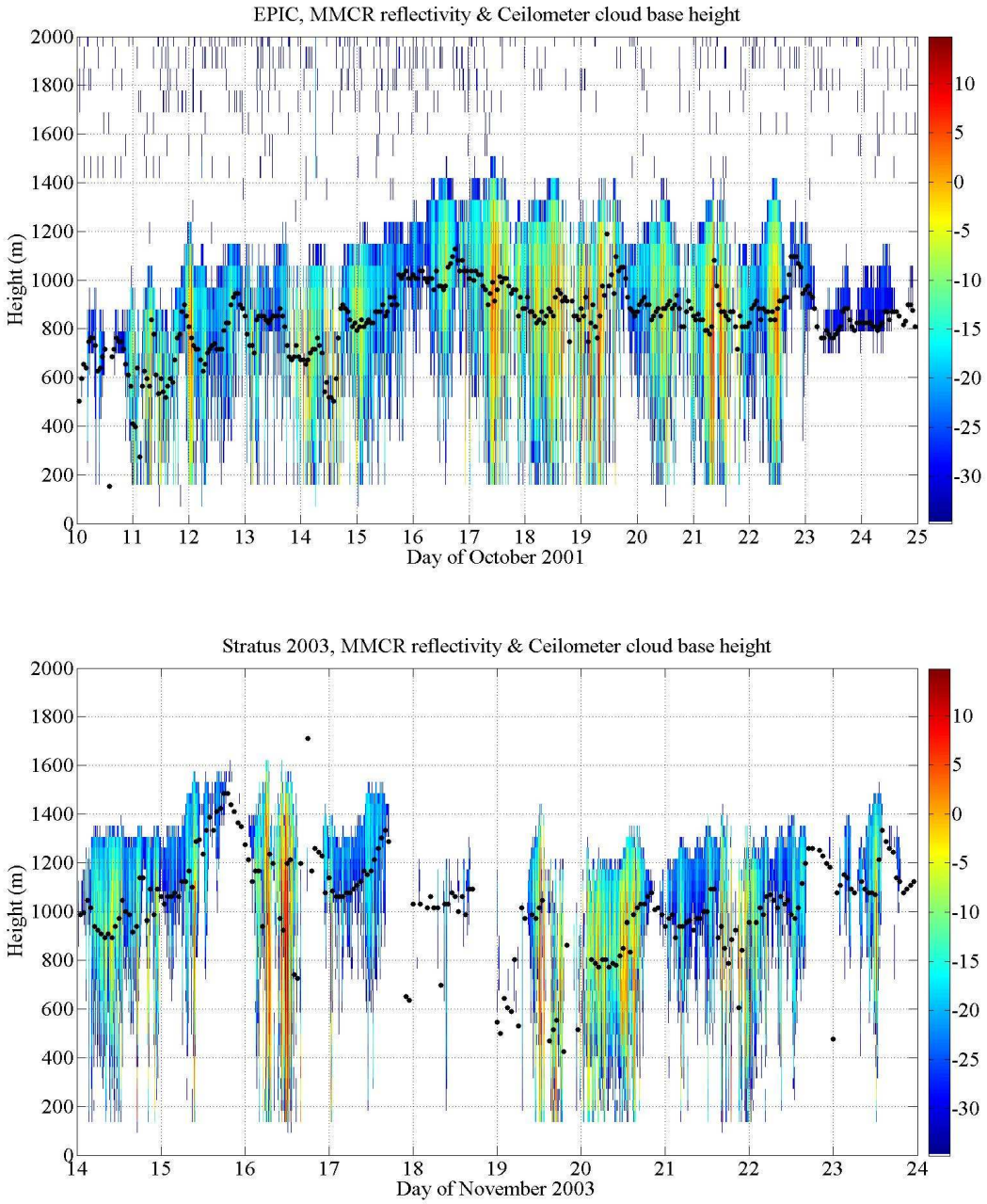

Figure 3.10: Reflectivity from the MMCR during EPIC 2001 (top) and Stratus 2003 (bottom). The ceilometer cloud base height is shown with the black dots.

The data illustrate the variability of marine stratus occurrence over the length of the two cruises. There are periods of continuous cloud coverage, especially during the EPIC 2001 cruise, and clear-sky periods, especially during the Stratus 2003 cruise. The cruise-averaged cloud fraction was about 92% and 82% for EPIC 2001 and Stratus 2003 respectively (80% for Stratus 2004). The presence of radar returns below the ceilometer cloud base indicates drizzling periods. During EPIC 2001, the cloud top exhibits large diurnal variability (150-200 m) while the cloud base shows less diurnal variability, although the range of variations is still 800 to 1000 m. Drizzle was observed frequently during nighttime and early morning hours, when the cloud layer was thick and contained high values of liquid water. During Stratus 2003, the striking feature is the presence of extensive periods of clear skies especially at the buoy location. Furthermore, the cloud base height exhibits higher variability, and the drizzle occurrence was lower. In both cruises, the cloud base rises during the early morning hours and soon after the marine stratus cloud thins or dissipates.

Radar reflectivity was used to extract the hourly drizzle occurrence during each cruise. The threshold value used to identify drizzle is maximum radar reflectivity in the column greater than -10 dBZ (Frisch et al. 1995a). The classification allows the calculation of the hourly drizzle fractional coverage, which is defined as percent of profiles that contain drizzle (according to the reflectivity threshold) within each hour. Figs. 3.11 and 3.12 show the time series of hourly estimates of cloud and drizzle fraction during the three cruises.

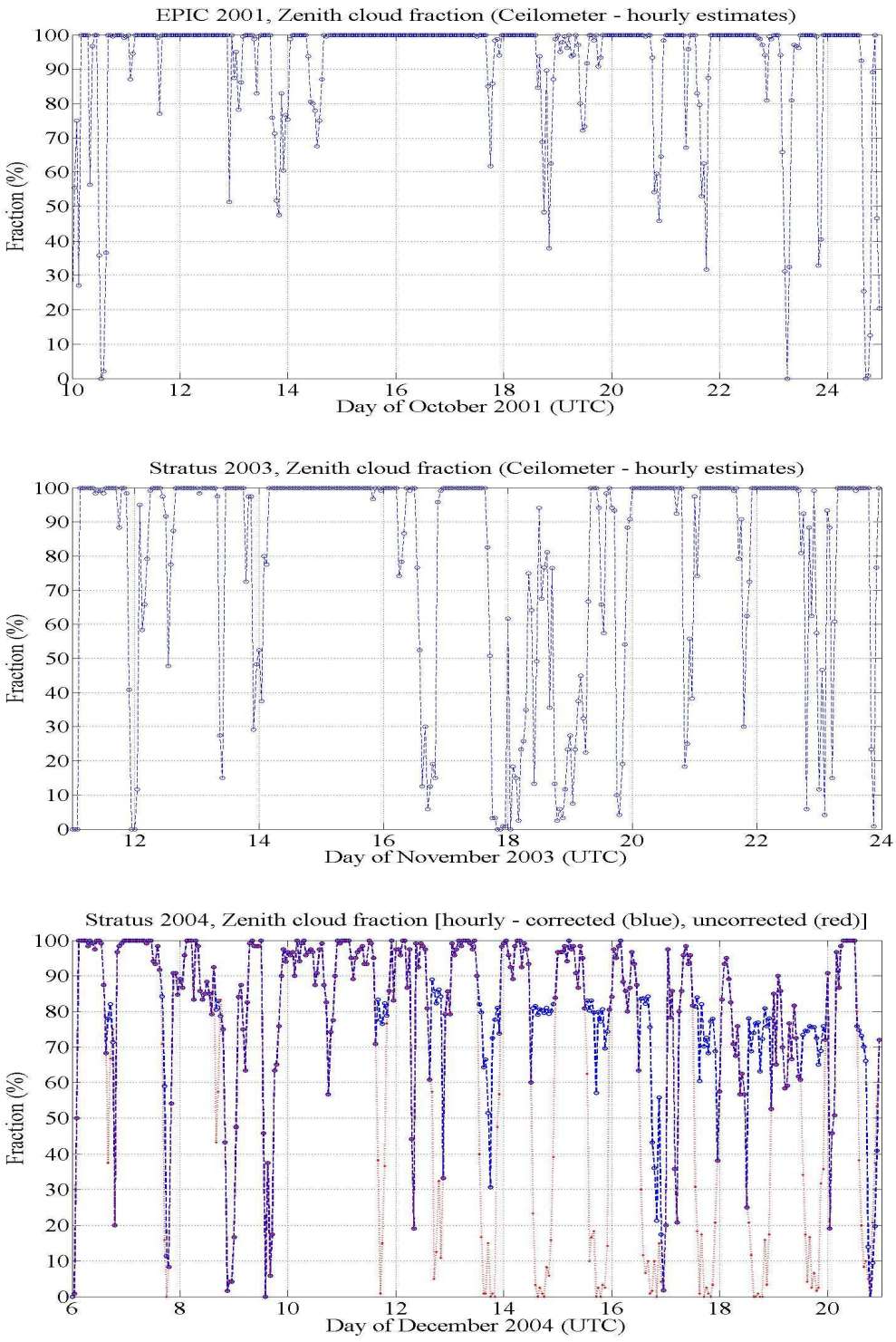

Figure 3.11: Hourly estimates of zenith-point fractional cloudiness from the ceilometer for EPIC 2001 (top), Stratus 2003 (middle) and Stratus 2004 (bottom). During Stratus 2004, the daytime cloud fraction values were adjusted using the observed downward longwave radiation (blue circles). The uncorrected values are also displayed (red dots).

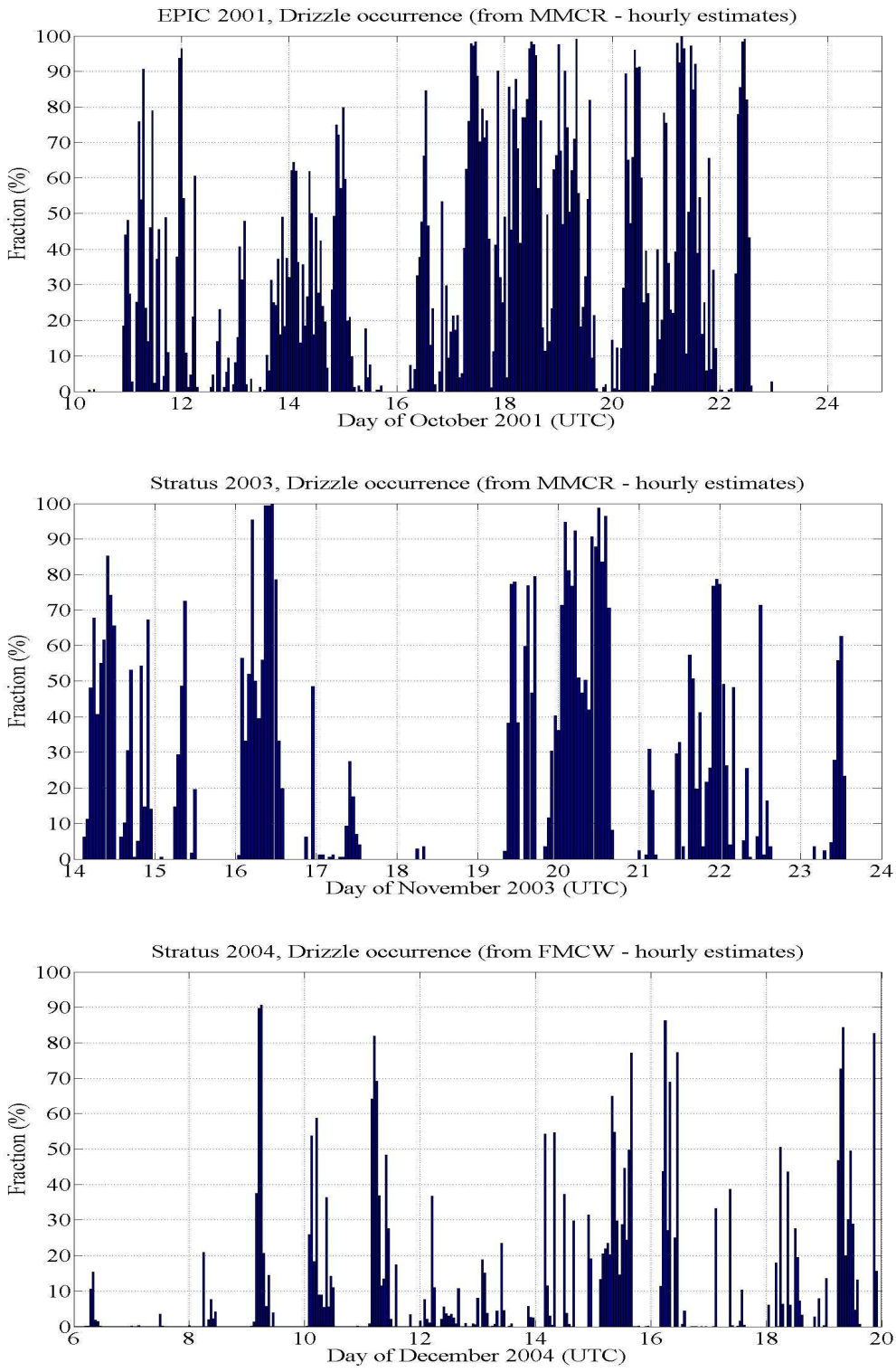

Figure 3.12: Hourly fractional drizzle occurrence for EPIC 2001 (top), Stratus 2003 (middle) and Stratus 2004 (bottom). Drizzle is defined as MMCR (for EPIC and Stratus 2003) or FMCW (for Stratus 2004) radar profiles having maximum (column-integrated) reflectivity greater than -10 dBZ.

The indication of a possible reduction in cloud cover during the characteristic EPIC (October 18-19 and 21) and Stratus 2003 (November 16, 19 and 20) buoy period events, as mentioned in the previous section, is verified in Fig. 3.11; Indeed the respective periods are accompanied or followed by reduced cloud fraction (as measured by the ceilometers). In addition, extensive drizzle also occurs during or before these periods (Fig. 3.12), implying a mechanism of marine stratiform cloud dissipation that has been proposed by many studies in the past (e.g., Albrecht 1989); Drizzle evaporates below cloud base, and the resulting evaporative cooling stabilizes the boundary layer and inhibits surface turbulent fluxes from reaching the cloud layer. As a result, the cloud base rises and the clouds get thinner or even dissipate, leading to broken-sky areas and reduced cloud cover.

The EPIC 2001 cloud fraction values show little or no sign of diurnal variability. Overall, overcast conditions were observed, with large fraction of drizzle occurrence during the nighttime. The drizzle fraction exhibits diurnal variability with a maximum during nighttime. The Stratus 2003 and Stratus 2004 cloud fraction temporal evolution is different with a much stronger diurnal cycle. During Stratus 2003, extensive clear-sky periods were documented by the MMCR and the ceilometer while the research vessel was stationed at the WHOI buoy. During this period (i.e. November 17-19, 2003), the cloud fraction remains below 100% during nighttime. In Stratus 2004, the cloud fraction oscillates from 100% during the nighttime to much lower values during the daytime and particularly near the solar maximum period. During the same cruise the lowest drizzle fraction is observed. Comparing all three cruises, a relatively high cloud fraction is observed during EPIC 2001, despite the high nighttime drizzle occurrence. Although

drizzle is thought to have a stabilizing effect on the MABL, the MABL during EPIC 2001 maintained a well mixed state and the clouds persisted throughout the cruise.

The liquid water path is another important cloud variable. The LWP is proportional of the cloud depth. Typically through the cruises, when the cloud thickness exceeds 200-250 m and the LWP exceeds 200 g/m^2, drizzle formation is favorable. Accurate measurements of LWP are of fundamental importance for the retrieval of the radiative properties (e.g., optical depth) of clouds. During the EPIC 2001 and Stratus 2003 cruises the NOAA/ETL microwave radiometer is used to retrieve the LWP from the observed brightness temperatures at 21 and 31 GHz. The retrieval of the LWP is suspect to biases and errors introduced in the physical retrieval by uncertainties in the radiative transfer model and uncertainties related to calibration. Zuidema et al. (2005) describe a technique used for the correction of the microwave radiometer measurements during the EPIC 2001 cruise. A similar correction technique was applied to a reduced portion of the Stratus 2003 data set (November 18-23). Fig. 3.13 shows the corrected 10-min averaged LWP time series during the two cruises, kindly provided to us by Dr. Zuidema. During EPIC 2001, at the buoy location, the LWP was dominated by a strong diurnal cycle that was not apparent in the cloud fraction time series for the same period from the ceilometer. This is consistent with a diurnal variation in cloud depth due to the cloud top variability. The maximum LWP values reach or exceed 300 g/m^2 during nighttime, when the stratus deck has maximum thickness and drizzle droplets form. We should note that the amount of liquid water distributed in drizzle size droplets never exceeds the 10% of the total cloud liquid water content. During daytime, the LWP drops to 30-50 g/m^2. The same range of LWP values is observed during the Stratus 2003 cruise, although, the signature of a

strong diurnal cycle is interrupted by the presence of extensive time periods with clear skies.

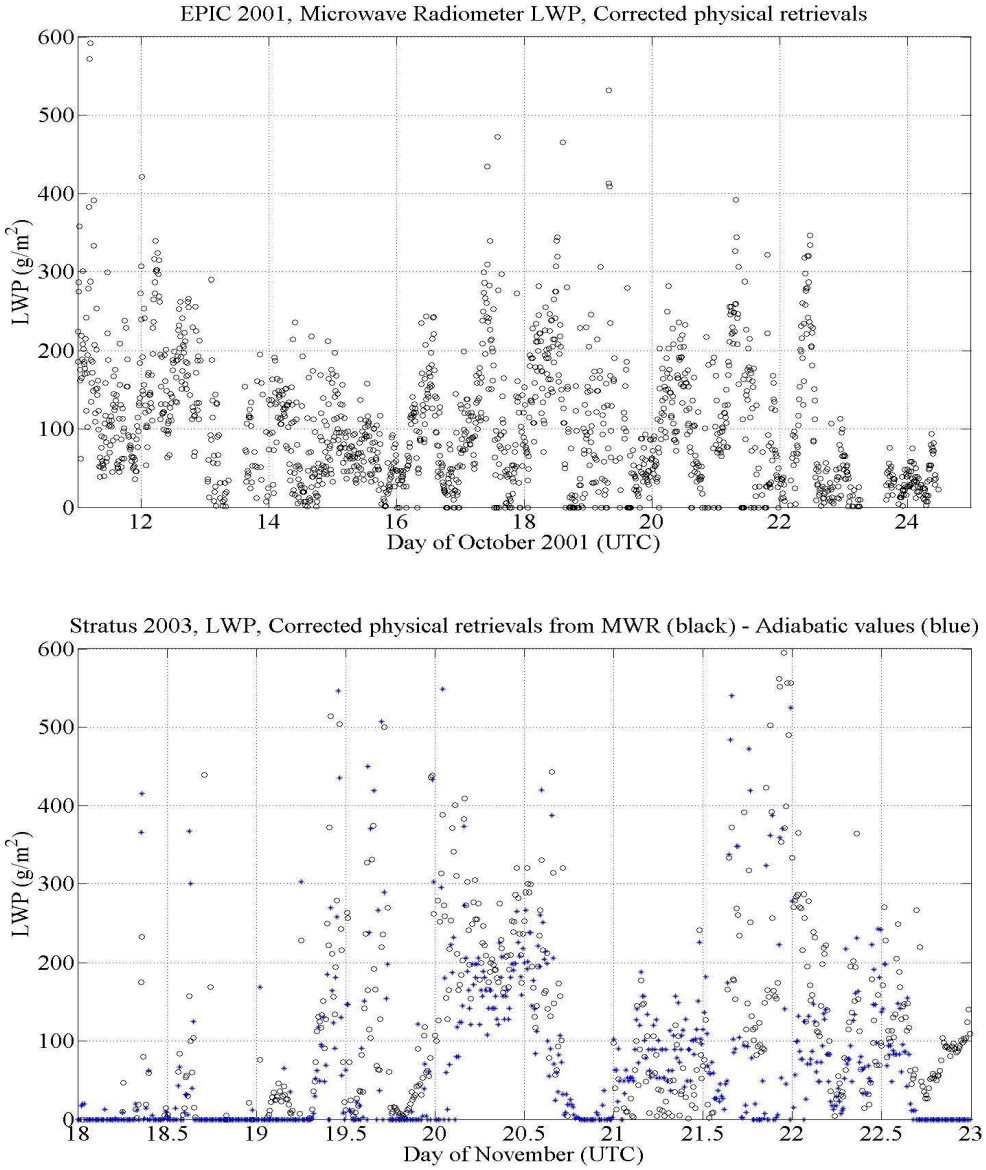

Figure 3.13: Top: EPIC 2001 time series of LWP from the microwave radiometer onboard the *Brown*. Values were retrieved at 10-min intervals from the corrected brightness temperatures, following Zuidema et al. (2005). Bottom: Time series of the physically retrieved (black) and the adiabatic values (blue) of LWP for the Stratus 2003 period of November 18-23. Data were kindly provided by Dr. Zuidema.

3.3 Diurnal Variability

Strong surface fluxes and cloud top IR cooling are the primary mechanisms that keep the MABL well mixed and maintain the marine stratus deck near the top of the boundary layer during nighttime. During daytime, the absorption of solar radiation near the cloud top partially offsets the IR cooling and thus reduces the turbulence kinetic energy that promotes vertical mixing and supplies the stratus deck with moisture. As a result, the cloud layer can partially thin or completely evaporate leading to clear-sky periods (e.g., Miller and Albrecht 1995; Wood et al. 2002). This diurnal cycle of cloud coverage and drizzle occurrence in the SE Pacific is the focus of this section. The diurnal cycle signature is often disturbed by synoptic and large scale features such as inertia-gravity waves (Bretherton et al. 2004), and fluctuations in the subsidence rate at the top of the MABL.

Using the cloud- and drizzle-fraction hourly estimates reported in the previous section we construct the diurnal cycle of cloud and drizzle occurrence for the three cruises (Fig. 3.14). In general, drizzle occurrence seems to vary diurnally in accordance with fractional cloudiness in all three cruises. As we discussed earlier, the EPIC 2001 diurnal cycle of cloud and drizzle amount is relatively weak compared with the subsequent cruises. The highest values of cloud and drizzle fraction are observed during the night and early morning hours. Cloud fraction values remain remarkably high (above 90%) almost for the entire day, i.e. from early evening (1700 local time; LT) to late morning (1000 LT). Even at local noon cloud fraction does not drop below 80%. Drizzle occurrence shows

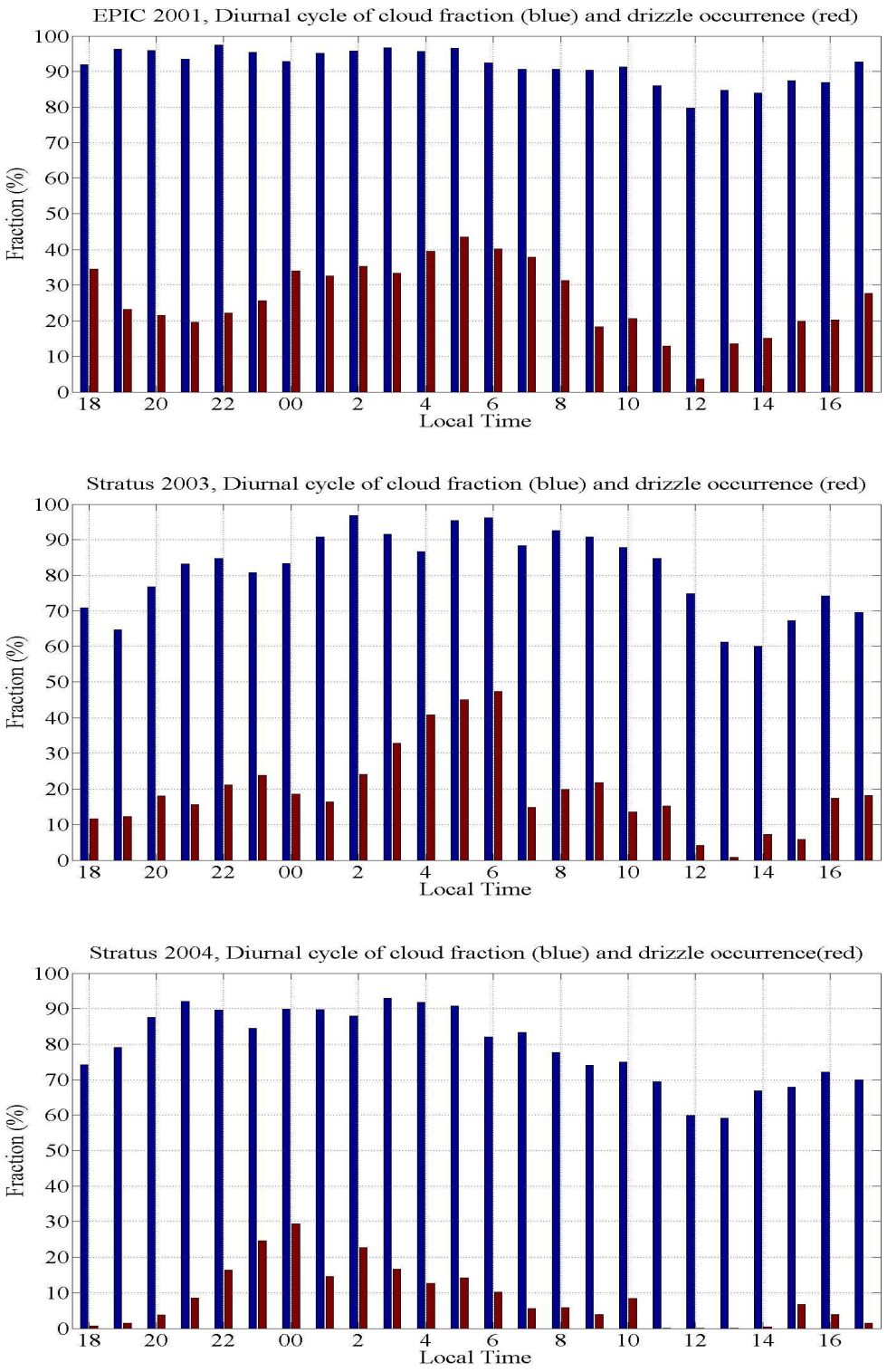

Figure 3.14: Diurnal cycle of cloud (blue) and drizzle (red) fraction during EPIC 2001 (top), Stratus 2003 (middle) and Stratus 2004 (bottom). A -10 dBZ reflectivity threshold is used in the MMCR/FMCW data for the retrieval of the drizzle fraction. The corrected ceilometer data are used for extracting the Stratus 2004 cloud fraction diurnal cycle.

higher diurnal variability than cloud fraction during the EPIC cruise, with a distinct maximum at 0500 LT (44%) and a minimum at local noon (3%). During Stratus 2003, the cloud and drizzle fraction demonstrate higher diurnal variability. The maximum values of cloud and drizzle fraction are observed at 0600 LT (98% and 48% respectively) and the minimum values are observed right after local noon (60% and 1% respectively). Stratus 2004 is also characterized by pronounced diurnal variability in cloud fraction with higher values during nighttime and lower during daytime compared with Stratus 2003. The maximum cloud fraction value was recorded at 0300 LT (93%), whereas the maximum in drizzle occurrence was recorded a few hours earlier (30% at local midnight). The lowest cloud fraction values also occurred at 1200 and 1300 LT (60%), when the clouds had no drizzle in or below the cloud layer. Drizzle occurrence during Stratus 2004 shows a different diurnal variation compared with that on the earlier cruises; this may be attributed to the difference in boundary layer structures and cloud regimes between the three research cruises.

3.4 Inversion Layer Characteristics

Across the MABL capping inversion layer, the potential temperature θ increases and the mixing ratio r decreases rapidly with height. These changes in θ and r across the capping inversion are generally much larger than the changes observed from the surface to the base of the capping inversion, and thus are not difficult to detect with the use of a proper thermodynamic property-based gradient technique across the vertical structure of

the MABL as it is documented by the soundings. In this study the parameter μ is used (Yin and Albrecht 2000) that is given by:

$$\mu = \beta \frac{\partial r}{\partial p} - \frac{\partial \theta}{\partial p},$$

where p is the pressure level (mb), and β is a parameter given by:

$$\beta = \frac{0.608\theta}{(1 + 0.608r)}.$$

The parameter β is used to convert the gradient of the mixing ratio to the same units as the gradient of the potential temperature. In this study, the parameter μ is estimated for each sounding available and time-height maps of μ are produced for each cruise (Fig. 3.15). Before μ is estimated, a low pass filter is applied to the profile of the potential temperature and mixing ratio to remove spurious effects and outliers. The inversion layer is clearly indicated by a local maximum of μ (values from 0.5 to 2.5). Using a subjectively-selected threshold value of μ (0.3), the upper and lower boundaries of the capping inversion were retrieved (as the nearest heights that corresponded to a value of μ=0.3 above and below the maximum value, respectively) along with the corresponding values of potential temperature and mixing ratio. Thus, using this methodology, the gradients of θ and r across the inversion and the inversion strength were calculated. The retrieved MABL capping inversion base shows great agreement when compared against the retrieved cloud top from the MMCR. Typical $\Delta\theta$ values for all three cruises were between 5 and 15 K. The gradient of the mixing ratio Δr across the inversion varies between -2 and -8 g/kg.

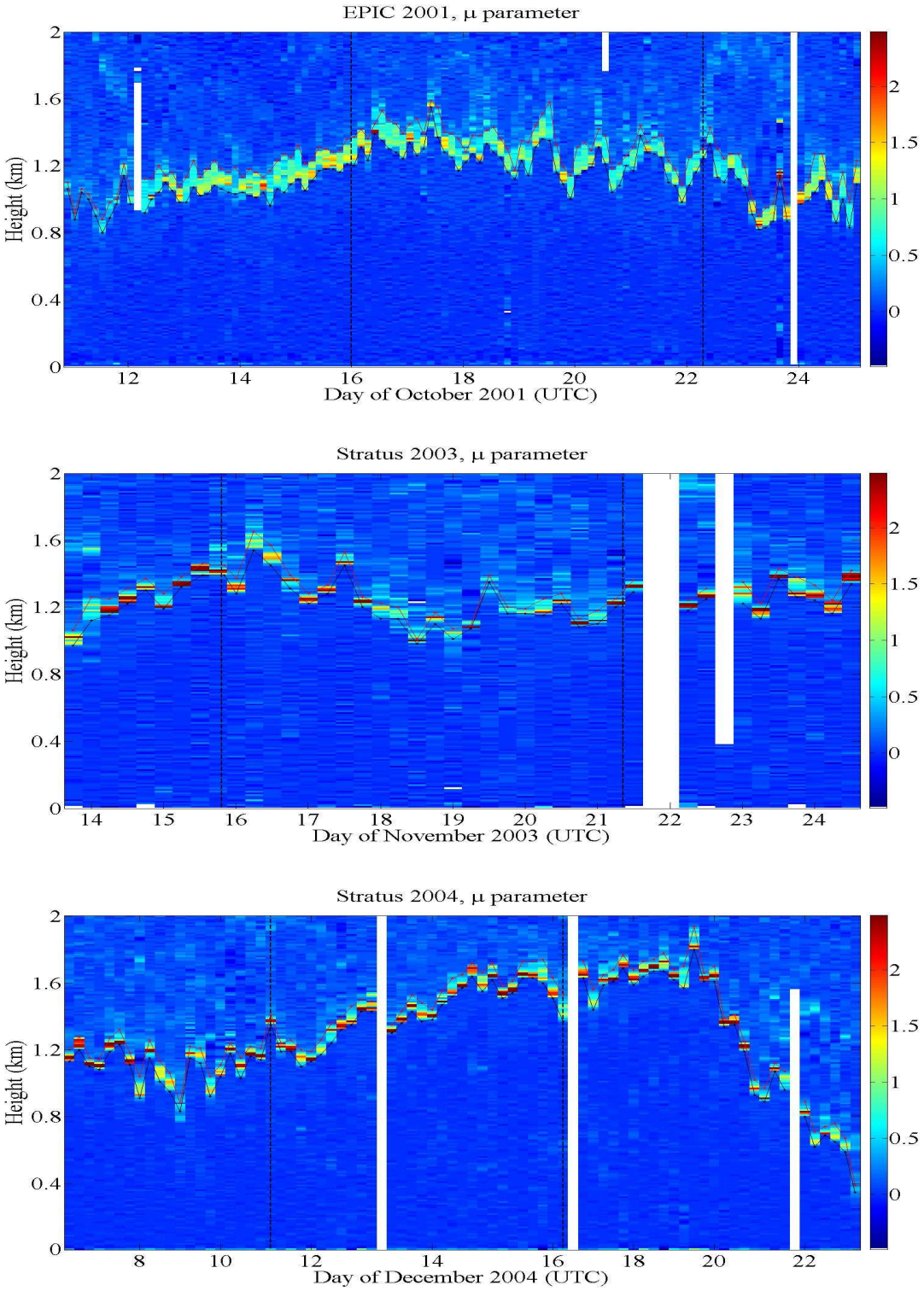

Figure 3.15: Time-height mapping of the parameter μ from the soundings during EPIC 2001 (top), Stratus 2003 (middle) and Stratus 2004 (bottom). Dashed lines indicate the period when the ship was stationed at the WHOI buoy; white segments indicate missing or bad sounding values.

In addition to the gradients of potential temperature and mixing ratio, the physical thickness of the capping inversion was estimated using the same technique. On average, for all three cruises the physical thickness of the inversion was between 50-200 m. The larger values of inversion thickness were observed during the EPIC 2001 cruise with a large number of soundings that show thickness values higher than 100 m. During the Stratus cruises the thickness was between 50-100 m.

Chapter 4 – Buoy Period Observations

4.1 Introduction

Chapter 3 provided a descriptive and comparative view of the boundary layer, cloud and drizzle evolution throughout each cruise. Temporal and spatial similarities and differences between the three cruises were addressed. Three domains were mainly taken into account, namely the southward route that marked the beginning of the EPIC and Stratus 2003 cruises, the period that the ships were stationed at the Stratus ORS location (20°S, 85°W), and the 20°S transect from the buoy location to the coast of Northern Chile. The 5 to 6-day buoy periods provide an opportunity to focus on the observations at a specific geographical location and eliminate the spatial variability arousing from the different ship tracks. Thus, it appears to be the most suitable domain for giving a climatological perspective to the current study; it favors the extraction of average thermodynamic and dynamical profiles (from the soundings) as well as an estimate of mean- and standard deviation values of most macrophysical properties associated with boundary layer structure and cloudiness in the SE Pacific.

4.2 Mean and Variance Thermodynamic Profiles

Mean vertical profiles for the MABL thermodynamic and dynamical variables were constructed from the soundings launched during the EPIC (October 16-22), Stratus 2003 (November 16-21) and Stratus 2004 (December 11-16) WHOI buoy periods (Figs. 4.1

and 4.2), following the analysis techniques described in section 2.3. Geometric height is used in Fig. 4.1, in contrast to Fig. 4.2 that is plotted using height scales normalized by the inversion base height.

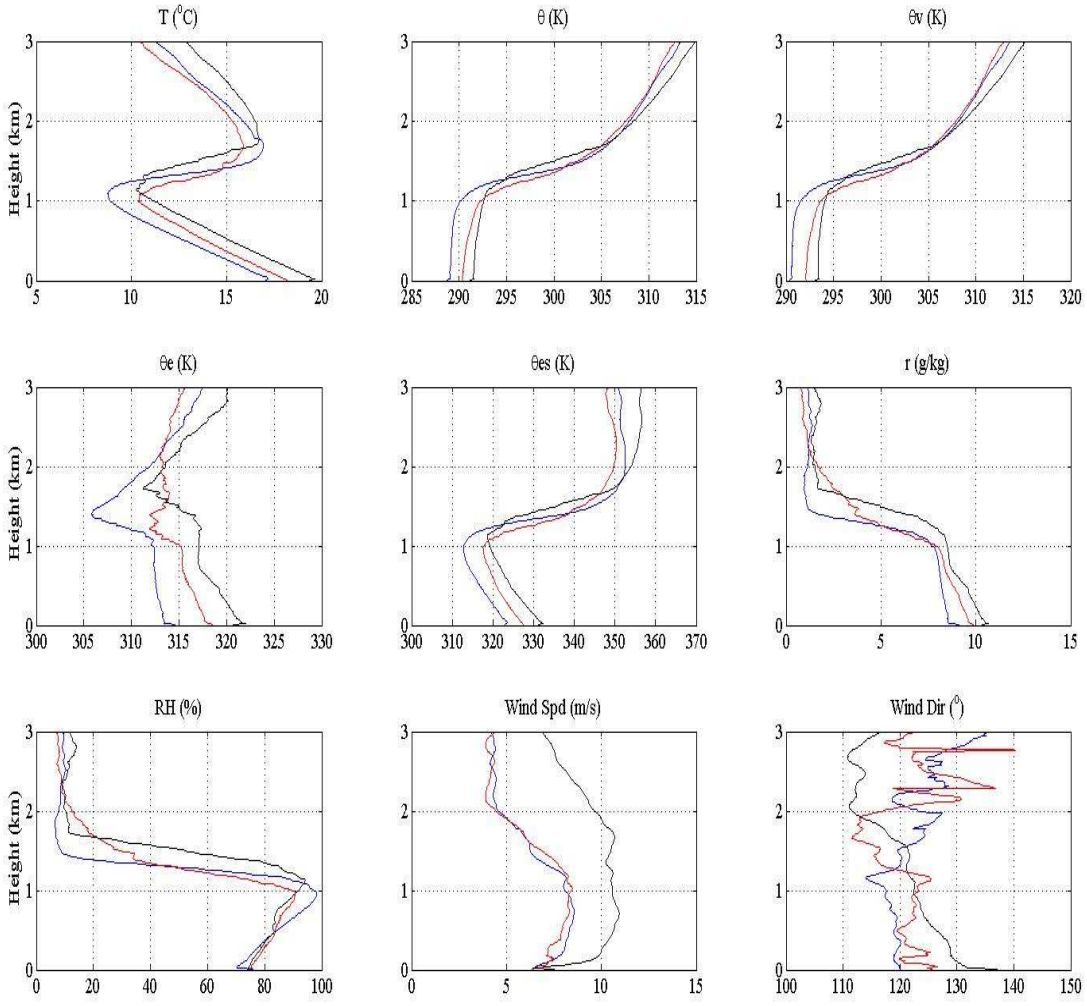

Figure 4.1: Mean profiles derived from the soundings launched during the 3 WHOI buoy periods: EPIC (blue) [6 days, October 16-22], Stratus 2003 (red) [5 days, November 16-21] and Stratus 2004 (black) [5 days, December 11-16]. Each variable is noted at the top of each subplot.

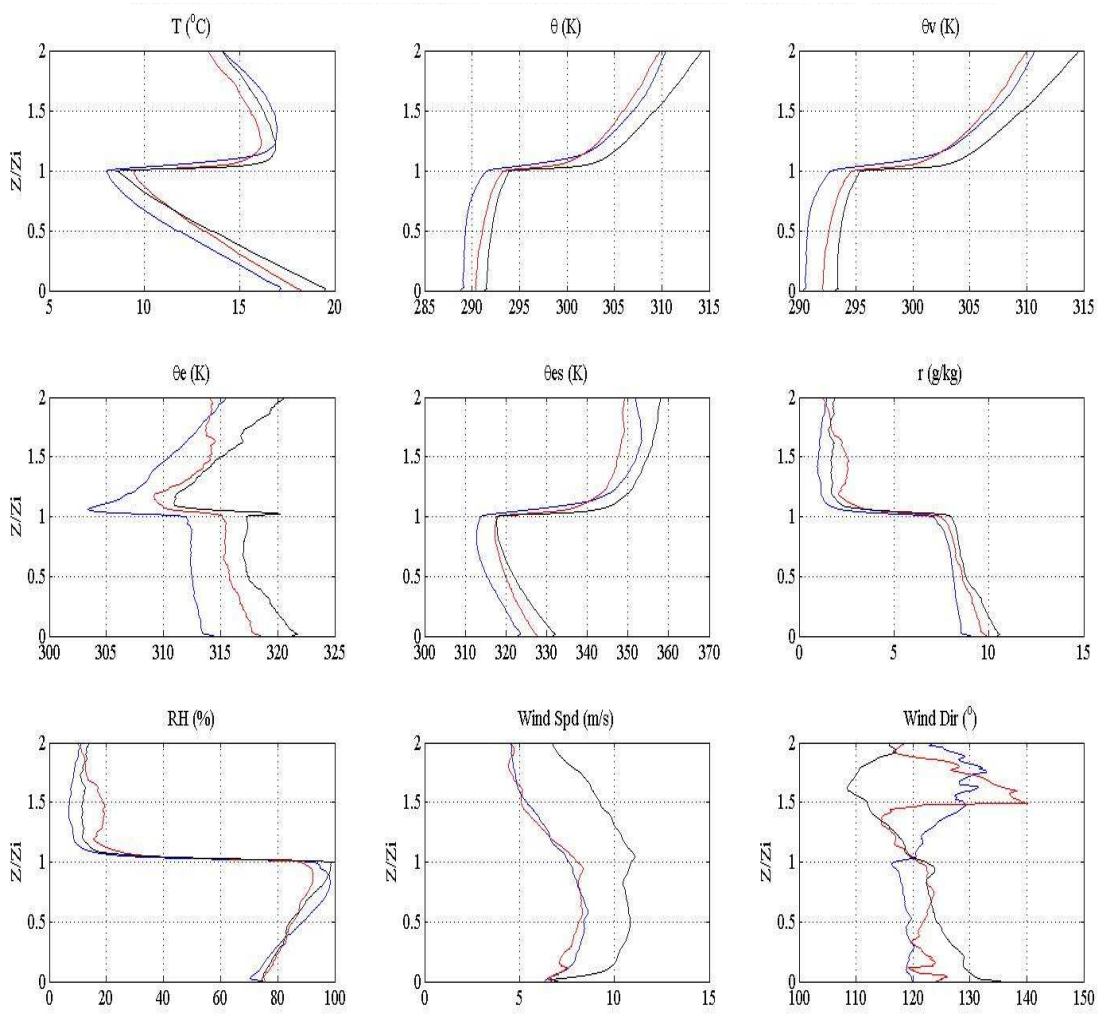

Figure 4.2: As in Fig. 4.1, but using height scales normalized by the height of the inversion z_i.

The temperature structure is quite similar for the three composite soundings, and shows the typical characteristics of a stratocumulus-capped marine boundary layer (nearly well-mixed in the subcloud layer and moist adiabatic in the cloud layer; a strong capping inversion with an exponential θ profile above the inversion). The differences observed seem to be consistent with the changes in SST. The mean SSTs are 18.6, 19.2 and 19.5°C for the EPIC-, Stratus 2003- and Stratus 2004 buoy periods respectively (see

Table 4.1 in section 4.4). The differences in SSTs are reflected in the boundary layer temperatures; the Stratus 2003 buoy-period boundary layer is about 1-2°C warmer than EPIC, and the boundary layer during the Stratus 2004 buoy period is even warmer by about 0.5-1°C (Figs. 4.1 and 4.2, θ profile).

The difference in boundary layer regimes encountered during the three buoy periods (section 3.2.1) is mostly reflected in the composite mixing ratio soundings. The EPIC composite sounding is fairly well mixed, showing only a very small gradual decrease in mixing ratio from the surface to the inversion base height. The Stratus 2003 buoy-period sounding is moister than EPIC, especially in the lower boundary layer. From the surface to about 500 m, mixing ratio decreases slightly with height similarly to the EPIC sounding, but above 500 m it demonstrates a higher decrease rate, which is indicative of the partially decoupled conditions observed intermittently during the 2003 buoy period. The same structure is observed in the Stratus 2004 composite sounding as well, although this sounding is even moister and more decoupled than Stratus 2003 (Figs. 4.1 and 4.2, r profile). Both 2003 and 2004 soundings are characteristic of the existence of a second cloud base (shallow cumuli clouds) below the stratocumulus. The base of the cumuli clouds is marked by the transition layer in the two composite soundings. The height of this layer is at 0.35 z/z_i, which corresponds to a geometric height of 500 m. This is consistent with the respective heights measured for the NE Pacific stratocumulus regime during the First International Satellite Cloud Climatology Project (ISCCP) Regional Experiment (FIRE; 1987), and the Atlantic stratocumulus-to-cumulus transition regime that was the focus of the Atlantic Stratocumulus Transition Experiment (ASTEX; 1992) (Albrecht et al. 1995a). A further conclusion following Albrecht et al. (1995a) is that the

height of the transition layer does not scale by the depth of the boundary layer, since the detailed structure of the transition layer is not preserved in the composite soundings. The middle and lower panels of Fig. 3.1 show that the LCL, calculated by surface values of temperature and mixing ratio, closely matches the height of the transition layer. In addition, a surface layer of about 50 m is indicated in all composite soundings.

The variations in mixing ratio profiles are also consistent with the changes in SST, since the relative humidity near the surface remains relatively constant (Figs. 4.1 and 4.2, *RH* profile). The relative humidity profiles below 500 m (height of the transition layer for the Stratus 2003 and 2004 buoy periods) are similar for the three boundary layers with relative humidity increasing with height from a minimum of about 73% near surface. Above 500 m, however, relative humidity for the Stratus 2003 buoy period is substantially lower than that of the EPIC sounding, and this difference is about 10% (88 and 98% respectively) at the height of the stratocumulus cloud layer (1000-1100 m). Although the Stratus 2004 composite sounding shows more enhanced decoupling than Stratus 2003, the mean relative humidity of the stratocumulus cloud layer is higher (~93%), indicating a fairly solid cloud layer despite the persistent decoupling and the higher cloud bases.

The composite soundings in Fig. 4.1 show mean wind directions consistent with climatology, with winds in the lower 3 km blowing from the east-southeast in all three buoy periods (see also section 3.2.3). The southerly component of boundary layer winds is slightly stronger in Stratus 2003 compared with EPIC, and becomes even stronger during the 2004 buoy period, especially for the lower boundary layer. The composite wind speed soundings are consistent with an earlier description of the cruise-track wind

field evolution (section 3.2.3). The EPIC and Stratus 2003 buoy periods are characterized by an identical wind speed profile, with winds of about 7-8 m/sec in the boundary layer that weakened above the inversion. In contrast, during the Stratus 2004 buoy period, the mean winds were consistently 3-4 m/sec stronger for the entire lower tropospheric profile. Although these conditions are considered favorable for enhanced turbulent mixing within the boundary layer that would normally result in well-mixed temperature and moisture soundings, the extensive period of decoupled conditions does not show such influence. However, these strong winds may have enhanced entrainment of dry air above the inversion into the cloud layer, which could possibly explain to some extent the significant inversion height increase during the Stratus 2004 buoy period described in the previous chapter. Another contrasting feature is that the strong winds characterizing Stratus 2004 are not accompanied by an enhancement of the surface buoyancy fluxes or colder advection due to smaller sea-air temperature differences during this cruise. This will be further investigated in the following section.

The inversion structure is well preserved by the scaling technique used in this study (Fig. 4.2) following Albrecht et al. (1995a). The potential temperature profiles above the inversion show the characteristic exponential profile that was often observed in our individual soundings (graphs not shown here). This exponential profile creates a difficulty with respect to the identification of the inversion top, which can be overcome with the use of the mixing ratio non-dimensional profiles. According to those, the inversion top is between 1.1 and 1.2 z/z_i for all three buoy periods, and these non-dimensional heights correspond to about 1400 m for EPIC and Stratus 2003 and 1600-1700 m for Stratus 2004, as seen in Fig. 4.1. The EPIC mean inversion-top height is in

good agreement with the respective value included in Table 4.1 (mean and std inversion variables were calculated with the use of parameter μ), whereas the Stratus 2003 and 2004 mean inversion-top heights seem to be underestimated by about 100 m in the same table. A discussion of the sensitivity of these calculations to the choice of the threshold μ value will follow in section 4.4. The highest inversion strength (as indicated by $\Delta\theta$ and Δr) is observed in EPIC, and the lowest in Stratus 2003. This is consistent with both the geometric-height and non-dimensional soundings as well as with the mean values shown in Table 4.1. The inversion thickness (i.e. difference between inversion-top and inversion-base heights) is at the same levels for the EPIC and Stratus 2004 buoy periods, while Stratus 2003 maintained a thinner inversion.

The variability of the boundary layer structure associated with the composite soundings is illustrated by the standard deviation profiles shown in Fig. 4.3. The small standard deviation values in the boundary layer compared with those above the inversion indicate the strong influence of the surface layer on the boundary layer structure. As expected, the highest variability is associated with the inversion layer. In general, the three observational periods demonstrated similar variability with slight differences below and above the inversion. This could be indicative of the weak influence of the Stratus ORS location by synoptic-scale systems. For the temperature profiles, Stratus 2003 showed the most variable conditions in the boundary layer, which is consistent with our former description in section 3.2.1, and Stratus 2004 was the least variable. The Stratus 2004 buoy period was the most variable with respect to the inversion layer temperatures, which can be explained by the significant and rapid boundary layer deepening, also

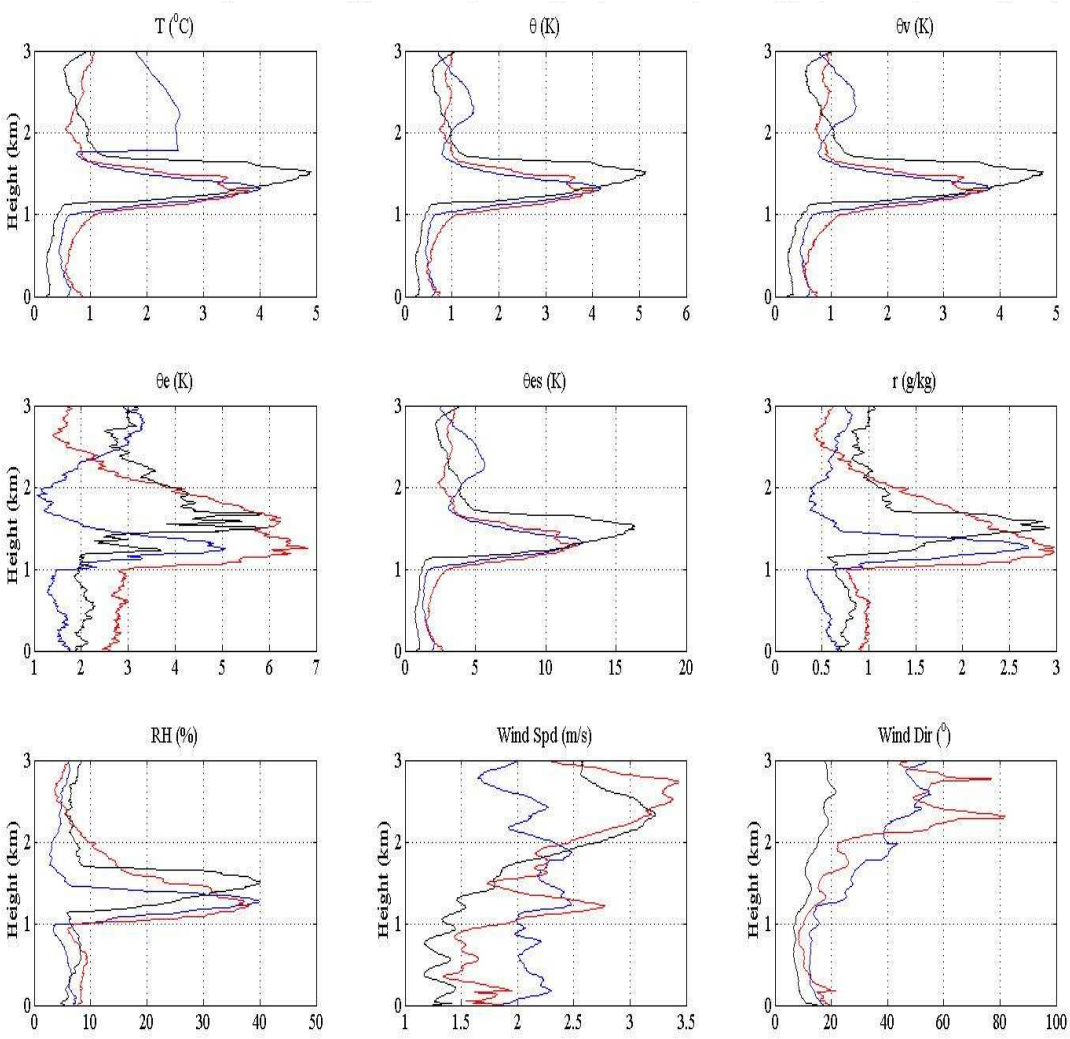

Figure 4.3: As in Fig. 19, but showing standard deviation profiles.

described in section 3.2.1. In contrast, EPIC temperatures showed the most variable conditions above the inversion. The moisture profiles indicate a rather different variability structure between the three buoy periods, with Stratus 2003 moisture values having the highest standard deviations for the entire low-tropospheric profile and EPIC being the least variable. Comparing our temperature and standard deviation profiles with

the respective profiles from the San Nicolas Island during FIRE – analyzed by Albrecht et al (1995a), – we observe that similar variability characterizes all profiles in the boundary layer, whereas above the inversion the FIRE profiles have larger variances compared with the EPIC/Stratus profiles. These large variances during FIRE were believed to be introduced by synoptic and mesoscale variability (Albrecht et al. 1995a). EPIC showed the highest variability in the boundary layer wind structure, whereas above the inversion Stratus 2003 was the most variable.

4.3 Mean Wind and SST fields

In addition to the SST, another important factor affecting boundary layer temperatures in the subtropical SE Pacific stratocumulus regime is temperature advection from the mean wind. To study this effect, mean surface wind and SST fields were plotted from NCEP reanalysis data (Kalnay et al. 1996) for the entire spatial domain sampled during the three field experiments. The 5- or 6-day mean SST and wind vector composites, shown in Figs. 4.4-4.6 for the three buoy periods respectively, were provided by the NOAA-CIRES Climate Diagnostics Center (CDC), Boulder, Colorado (CO), from their Web site at http://www.cdc.noaa.gov. These plots also allow for a comparison of our data sets with NCEP reanalysis data. For the location surrounding the WHOI buoy, the NCEP reanalysis mean SST, surface wind speed and wind direction values (Figs. 4.4-4.6) show good agreement with the respective mean estimates from the three buoy periods described in the previous section (Fig. 4.1 and Table 4.1).

The mean southeasterly wind direction, in association with the observed SST fields, suggests that the area around the Stratus ORS location is characterized by cold temperature advection. The SSTs to the southeast of the ORS location are colder during the EPIC buoy period – compared with the respective periods in Stratus 2003 and 2004, – but this is consistent with climatology, since EPIC took place in mid-spring, i.e. in a colder period for the Southern Hemisphere compared with the late spring occurrence of Stratus 2003 and early summer occurrence of Stratus 2004. This is also verified by the CDC 5-day SST anomaly plots (graphs not shown here). The eddy-like features close to the Chilean coast, observed in all three SST plots, may reflect localized upwelling/ downwelling areas or may be due to the low grid-point resolution of the NCEP Reanalysis data.

Using the netcdf data files provided by the CDC, we calculated the advective term of the surface temperature budget equation, given by:

$$\left(\frac{\partial T}{\partial t}\right)_{adv} = -u\frac{\partial T}{\partial x} - v\frac{\partial T}{\partial y}.$$

For these calculations, we used the mean zonal (u) and meridional (v) wind components, estimated by the buoy-period mean values of wind speed (V) and direction (φ) (Table 4.1) using the equations:

$$u = V\cos(\varphi)$$

$$v = V\sin(\varphi).$$

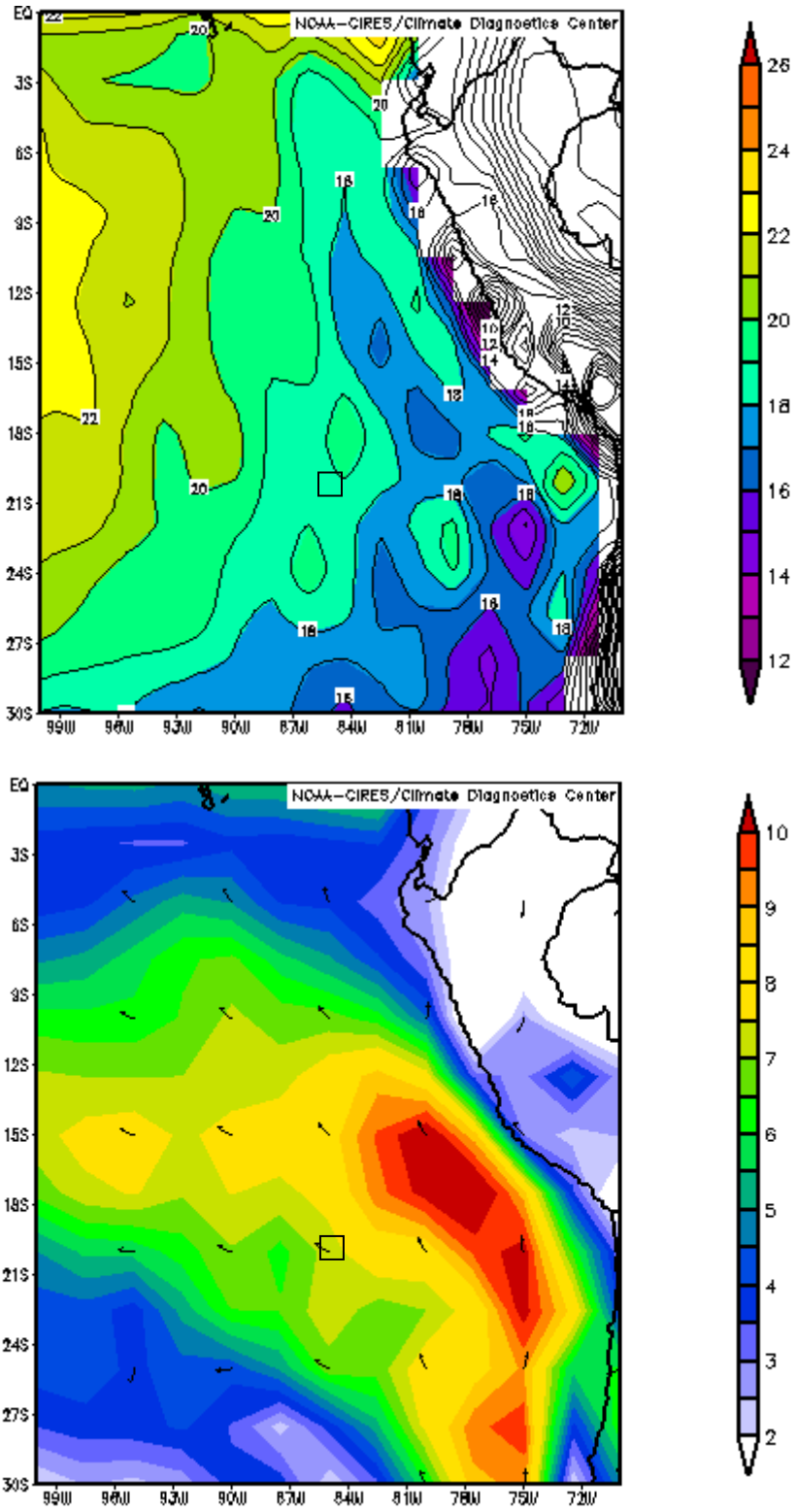

Figure 4.4: Daily mean composites of SST (top) and surface wind vector (bottom) from NCEP Reanalysis data for the 6-day EPIC buoy Period (October 16-22). Images provided by the NOAA-CIRES Climate Diagnostics Center (Boulder, CO) from their Web site at http://www.cdc.noaa.gov. The transparent squares indicate the Stratus ORS location.

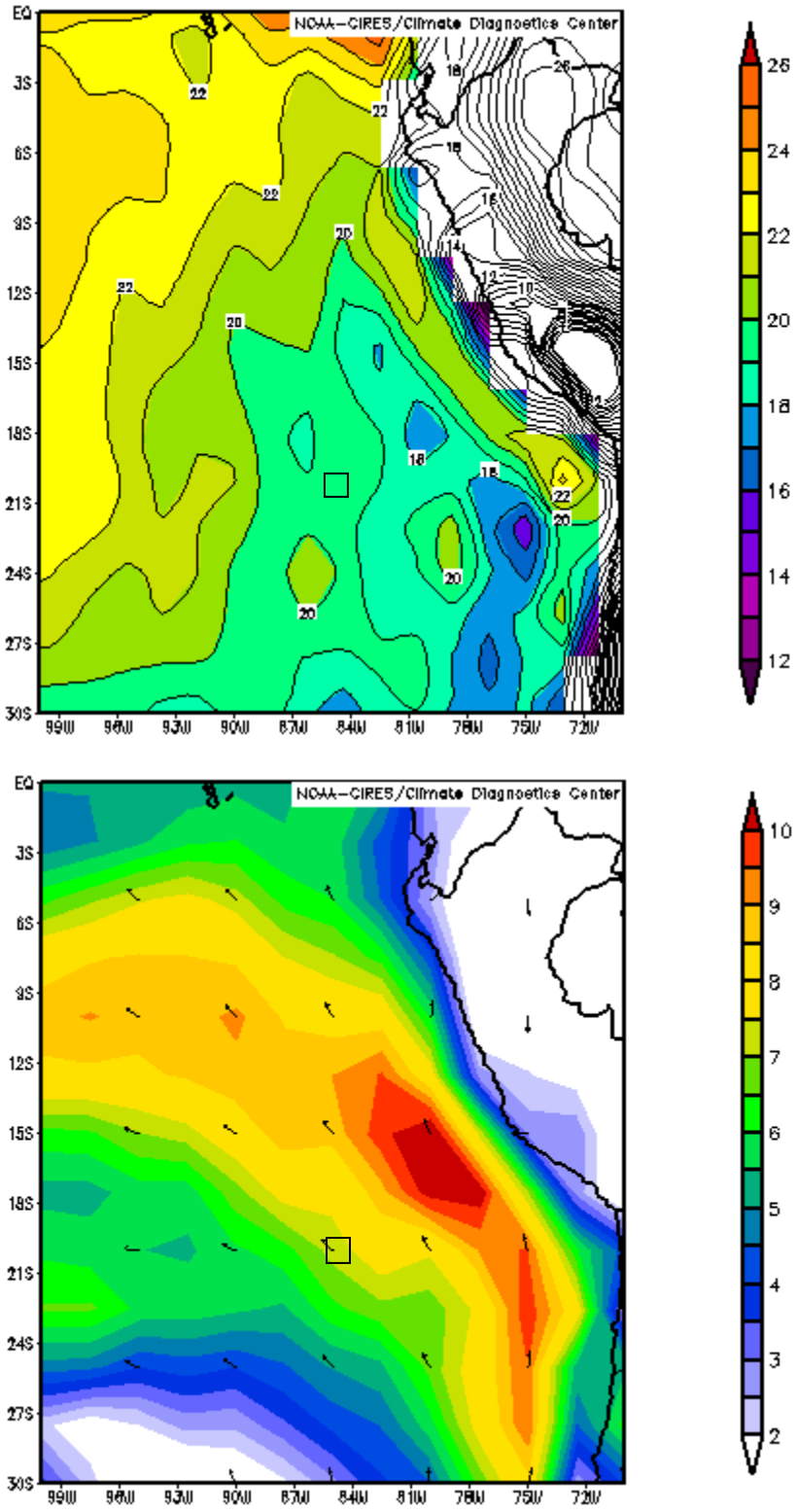

Figure 4.5: As in Fig. 22, but for the 5 days of the Stratus 2003 buoy period (November 16-21, 2003). Images provided by the NOAA-CIRES Climate Diagnostics Center (Boulder, CO) from their Web site at http://www.cdc.noaa.gov.

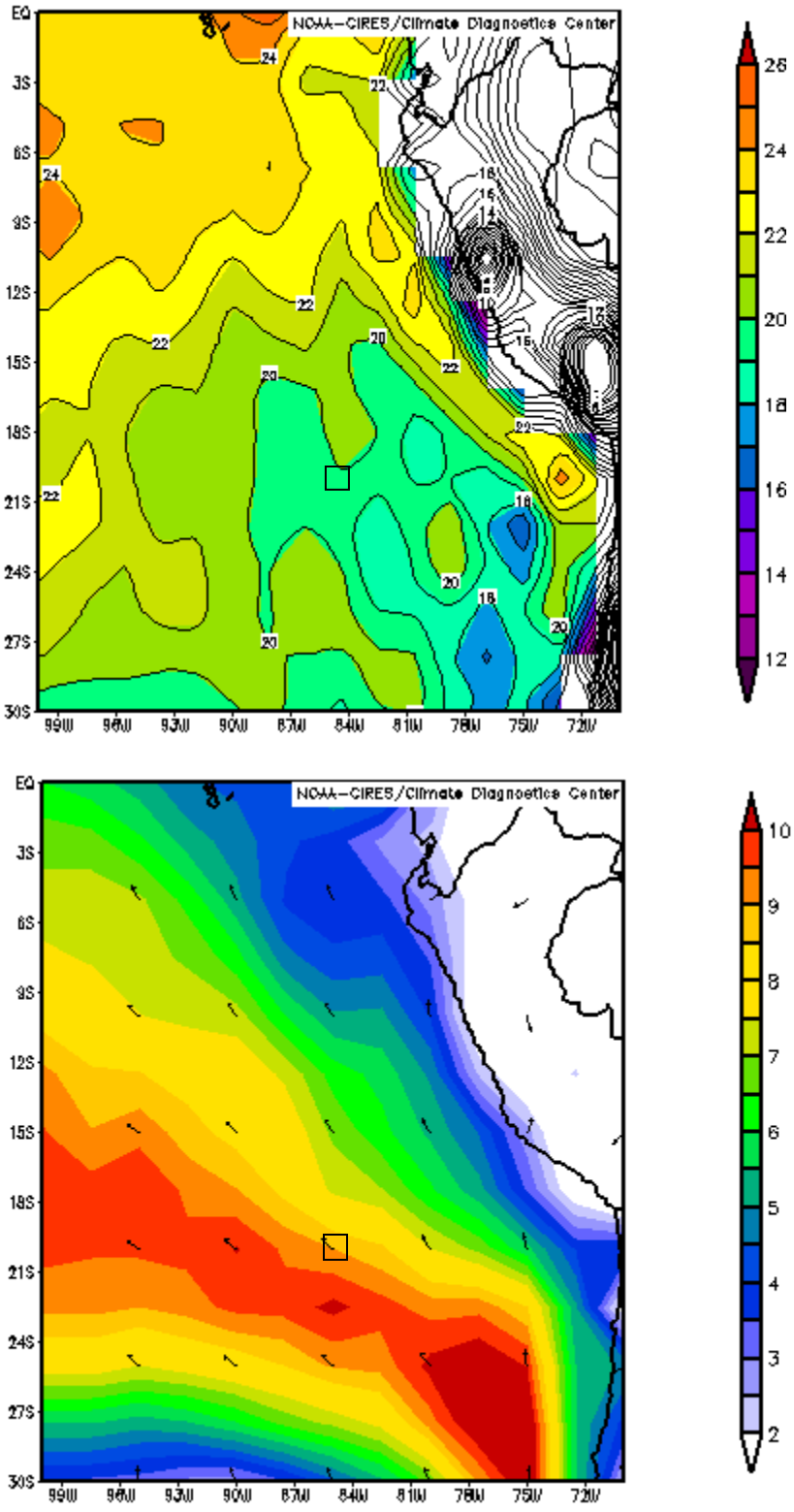

Figure 4.6: As in Fig. 22, but for the 5 days of the Stratus 2004 buoy period (December 11-16, 2004). Images provided by the NOAA-CIRES Climate Diagnostics Center (Boulder, CO) from their Web site at http://www.cdc.noaa.gov.

The zonal and meridional temperature (*T*) gradients were estimated with the use of grid-point SST values. The NCEP Reanalysis data, provided by CDC, had a resolution of ~1.9° in both latitude and longitude (each degree of latitude and longitude corresponds to a distance of about 111 km). The reference grid-point was chosen as the closest to the WHOI buoy location (20°S, 84.38°W), and the zonal (meridional) gradient was estimated with the use of the SST and longitude (latitude) difference between the reference grid-point and the grid-point located at 77°W (25.7°S). We have to note that the calculations are highly sensitive to the choice of grid-points, i.e. the distance from the WHOI buoy location that is used to estimate the SST gradients. The choice of the specific latitude (25.7°S) and longitude (77°W) is substantiated by the distance (600-800 km) that a typical southeasterly wind of 7-10 m/sec travels within a day. Further, the weekly Reynolds' SST analysis and the monthly reconstruction, used to extract the daily SST values through linear interpolation, induces non-negligible uncertainty to the NCEP Reanalysis SST data.

This methodology provided temperature advection values of -1.82, -0.55 and -0.35°C/day for the EPIC, Stratus 2003 and Stratus 2004 buoy-periods respectively. Thus, the EPIC buoy period was characterized by significantly colder advection compared with the other two field experiments. Moreover, the reduced cold advection during the Stratus 2003 and 2004 buoy periods could possibly explain the very low sea-air temperature difference and the resulting near-zero sensible heat flux values, observed during the respective periods (see sections 3.2.2 and 3.2.4 and Table 4.1).

4.4 Summary - Averages and Standard Deviations

Table 4.1 includes mean and standard-deviation values for the MABL, cloud and drizzle properties used in this study from the soundings, ceilometer, radars and air-sea flux system data. The period that the research vessels were stationed in the proximity of the ORS location is again considered as the temporal averaging domain. This table summarizes the description followed in chapters 3 and 4, and could be a good reference for scientists and researchers that focus their studies in the SE Pacific stratocumulus regime or intend to compare this regime with other areas dominated by stratocumulus clouds around the world. This information could also be used as baseline boundary layer and cloud structure for building and evaluating models as well as for testing boundary layer parameterizations.

The buoy-period soundings are used for the calculation of the means and standard deviations of all temperature, moisture and wind parameters for the surface- (1000 mb), inversion- and above-inversion (700 mb) levels. Although the threshold value (μ=0.3) – that was used to calculate the inversion top and base heights in section 3.4 – allowed for an accurate representation of the inversion layer time-height evolution (Fig. 3.15), it did not provide very accurate estimates of the inversion variables when compared with the mean thermodynamic profiles of Fig. 4.1. A wide range of values was tested, and μ=0.15 gave the most accurate results compared with the mean geometric-height thermodynamic profiles of Fig. 4.1 and the mean cloud-top heights estimated by the radars (Table 4.1). This value still induces some differences (e.g., the ones discussed in section 4.2 between the observed mean cloud-top heights from Fig. 4.1 and the mean cloud-top heights from

Table 4.1 that were calculated with the use of the μ parameter). However, this value best compensates between the mean thermodynamic moisture profiles shown in Fig. 4.1 and the radar-derived cloud-top estimates; a higher value would give results closer to the radar cloud-top heights and significantly different from the values seen in Fig. 4.1, whereas a lower value would have the opposite effect. The sensitivity of the inversion variables estimation to this threshold value of μ should be taken into account in future studies that plan to utilize similar methodology. Hourly estimates/averages of the ceilometer and radar data, and 5-min averages of the air-sea flux system data were used before extracting the buoy-period means and standard deviations for the respective properties. The mean EPIC cloud-top height was manually reduced by 100 m to account for the reduced height resolution of the MMCR that resulted in an apparent overestimation of this height (Kollias, personal communication). The same correction was applied earlier in Fig. 3.1. Further, the wind-profiler technique, used to compensate for the malfunctioning of the MMCR during the Stratus 2004 experiment, appears to slightly overestimate the inversion-base/cloud-top height (see also Fig. 2.2).

Table 4.1: Buoy period statistics.

			EPIC		Stratus 2003		Stratus 2004	
			Mean	*Std*	*Mean*	*Std*	*Mean*	*Std*
Soundings	Surface (1000 mb)	Temperature T (K)	289.1	0.6	290.4	0.6	291.6	0.3
		Pot. Temp. θ (K)	289.1	0.6	290.4	0.6	291.6	0.3
		Vir. Pot. Temp. θ_v (K)	290.6	0.6	292.1	0.6	293.4	0.3
		Eq. Pot. Temp. θ_e (K)	313.3	1.6	317.7	2.7	320.8	2
		Sat. Eq. Pot. Temp. θ_{es} (K)	321.5	1.8	325.9	2	329.9	1.1
		Mix. Ratio r (g/kg)	8.5	0.6	9.6	1	10.2	0.8
		Rel. Humidity (%)	74.4	6.5	76.9	8	76.1	6
		Wind Speed (m/sec)	7.7	2.2	6.8	1.7	9.7	1.3
		Wind Direction (°)	119	14	121	17	129	9
	700 mb	Temperature T (K)	283.7	0.6	283.1	1.1	285.2	1.2
		Pot. Temp. θ (K)	314.1	0.6	313.4	1.2	315.7	1.3
		Vir. Pot. Temp. θ_v (K)	314.3	0.7	313.6	1.1	316.1	1.3
		Eq. Pot. Temp. θ_e (K)	317.9	2.8	316.2	1.8	322.5	4.2
		Sat. Eq. Pot. Temp. θ_{es} (K)	350.1	2	348.1	3.9	355.9	4.7
		Mix. Ratio r (g/kg)	1.1	0.8	0.8	0.6	2	1.3
		Rel. Humidity (%)	9.6	6.5	7.4	6.3	15.9	10.2
		Wind Speed (m/sec)	4.5	2	4.8	2.2	6.4	2.5
		Wind Direction (°)	140	60	155	85	120	16
	Inversion	Inversion Base Height (m)	1218	105	1208	152	1403	163
		Inversion Top Height (m)	1403	123	1311	166	1521	168
		Inversion $\Delta\theta$ (K)	10.5	2.5	7.1	2.4	9.6	1.1
		Inversion Δr (g/kg)	-5.9	1.2	-4.5	1.9	-5.2	2.3
		Inversion shear (m/sec)	-0.78	1	-0.5	1.3	0	1.5
Ceilometer		Cloud Base Height (m)	922	88	953	230	1104	185
		Zenith Cloud Fraction (%)	94.1	-	66.1	-	86.5	14.9
Radar		Cloud top Height (m)	1255	113	1233	184	1474	170
		Drizzle Occurrence	42.9	34	22.3	33.2	10.6	18.2
Radar-Ceilometer		Cloud Thickness (m)	341	118	276	142	323	134
Air-Sea Flux System		*SST* (°C)	18.6	0.1	19.3	0.2	19.5	0.1
		SST-T_{air} (°C)	1.6	0.6	0.6	0.5	0.1	0.3
		Surf. Sea Spec. Hum. q_{sea} (g/kg)	13.1	0.1	13.6	0.2	13.9	0.1
		q_{sea}-q_{air} (g/kg)	4.1	0.6	3.3	0.9	3.5	0.6
		Surf. Incom. Solar flux (W/m^2)	223	323	288	377	202	281
		Surf. Incom. IR flux (W/m^2)	383	17	364	30	393	10
		Sensible Heat Flux (W/m^2)	14	7	2	5	-2	3
		Latent Heat Flux (W/m^2)	99	19	68	27	83	19
		Virtual Heat Flux (W/m^2)	21	7	7	5	4	3

Chapter 5 – Discussion and Future Work

5.1 Summary

Ship-based observations of marine stratocumulus clouds during the EPIC 2001 and the Stratus 2003 and 2004 cruises have been used to study the variability of the MABL and clouds in the SE Pacific. The EPIC 2001 field experiment was the first attempt to study marine stratus clouds in this regime using ship-based instrumentation (Bretherton et al. 2004). During the Stratus 2003 (Kollias et al. 2004) and Stratus 2004 (Serpetzoglou et al. 2005) cruises new observational data sets of marine stratus clouds were collected. Here, the observations from these three cruises are used to document the structure and variability of the MABL, clouds and drizzle, and provide a cohesive description of their differences and similarities. We anticipate that the findings presented will help in the design of future field programs (e.g., VOCALS 2007). Furthermore, the systematical comparison among the three cruises will provide a benchmark for the modeling community (e.g., Large Eddy Simulation (LES)), where modelers can test their parameterization schemes and representation of marine stratus clouds for a variety of MABL, surface and large-scale forcing conditions. Some of the main features observed during the three cruises are summarized below.

The EPIC cruise provided an unprecedented data set of SE marine stratocumulus clouds that had been previously sparsely observed at such resolution and detail. During EPIC 2001, the MABL was well mixed, resulting in small LCL variability. The cloud fraction was very high - nearly no clear sky periods were observed with high nighttime

drizzle occurrence and drizzle rates (Comstock et al. 2005). Drizzle evaporation resulted in measurable cooling and moistening of the subcloud layer as observed by the surface met instruments and the soundings. Despite the stabilization of the boundary layer induced by the evaporation of drizzle, the MABL maintained a well mixed vertical structure that helped maintain the cloud layer. Stratus clouds with cloud thickness greater than 250 m had drizzle below the cloud base. A strong diurnal cycle in cloud thickness, cloud top height and LWP of marine stratocumulus was documented at the WHOI buoy location. Overall, the EPIC 2001 observations of marine stratus revealed an omnipresent stratus deck, with little or no transition to other MABL regimes such as broken clouds and decoupled conditions. These conditions were not observed on the subsequent cruises.

The Stratus 2003 cruise provided another dataset of MABL, clouds and drizzle in the SE Pacific. During the Stratus 2003 cruise, moderate vertical gradients of potential temperature and mixing ratio that overlap with periods of small cloud fractional coverage, decoupled layers and shallow cumuli clouds were observed. Furthermore, during Stratus 2003 the LCL varies substantially with time in conjunction with MABL variability. Large periods of clear skies were observed at the WHOI buoy location, especially during the solar flux maximum. The stratus observed at the buoy location during Stratus 2003 revealed a different picture from the one captured during EPIC, with sharp transitions from solid cloud deck to broken cumuli, and large vertical gradients of thermodynamic properties (e.g., mixing ratio and virtual potential temperature) in the MABL.

During the Stratus 2004 cruise, the observed MABL, cloud, and drizzle structures showed similar features with those observed in Stratus 2003. However, the presence of

decoupled conditions in the MABL was more pronounced. Decoupled conditions are first observed during the third day that the *Brown* is stationed at the buoy location and persist during the southeasterly route that the *Brown* followed afterwards. The decoupled MABL conditions resulted in decrease of the cloud thickness and the intermittent presence of shallow cumuli clouds below the high stratocumulus cloud base. Another interesting feature observed during Stratus 2004 was the elevation of the MABL capping inversion. Although the Stratus 2004 composite sounding showed more enhanced decoupling than Stratus 2003, the mean relative humidity of the stratocumulus cloud layer was higher, indicating a fairly solid cloud layer despite the persistent decoupling and the higher cloud bases.

The previous discussion is indicative of the three different regimes of boundary layer structure and cloudiness that characterized the PACS/EPIC research cruises conducted so far in the remote southeast Pacific area. Although many detailed features observed during these cruises can be attributed to particular synoptic scale disturbances, there were several characteristics of the MABL, the cloud structure, and the occurrence of drizzle that were documented and compared in all three cruises. These include:

- Cloud boundaries, cloud fraction, drizzle occurrence and LWP exhibit strong diurnal cycle with maximum values during nighttime and minimum near the local noon time. Typical cloud thickness was between 150 and 300 m and the thickest clouds were observed during EPIC 2001. The buoy-period-averaged cloud fraction was high for EPIC (94%) and Stratus 2004 (86.5%), but significantly lower for Stratus 2003 (66%).Drizzle occurrence was substantially reduced during Stratus 2004.

- The depth of the MABL capping inversion is between 50 and 150 m, with an increase of potential temperature across the inversion of $\Delta\theta$ = 6-9 K, and a decrease in mixing ratio of Δr = 4-5.5 g/kg.
- Typical measured sea-air temperature differences are between 0 and 2°C. EPIC was characterized by large sea-air temperature differences (~1.5°C), in contrast to Stratus 2003 (~0.5°C) and Stratus 2004 (0°C). This was due to reduced cold-air advection in the proximity of the WHOI buoy location during the later cruises.
- In accordance with the observed sea-air temperature differences, the highest sensible and latent heat fluxes were observed during EPIC 2001 (99 and 14 W/m^2 buoy-averaged values respectively). Lower values were observed during Stratus 2003 and 2004 (2 and 68 W/m^2 and -1.8 and 83 W/m^2 respectively).
- Near-surface (1000 mb) relative humidity values were around 75% on average for the three cruises and the mixing ratio was between 8 and 10 g/kg near the surface.
- The wind direction during all three cruises was relatively persistent from the southeast (120^o) and the wind speed at the surface (1000 mb) was 7-10 m/sec on average for the three cruises. Stratus 2004 was characterized by stronger winds that resulted from the enhanced anticyclonic circulation during the same period. Evidence of the low-level jet off central Chile (Garreaud and Munoz 2005) during Stratus 2004 as well as possible indications of the shallow meridional circulation (Zhang et al. 2004) during EPIC and Stratus 2003 were documented in the observed wind structures.

- Mid-troposphere moisture features were observed by the soundings in all three cruises. These features propagate downward and reach the layer above the capping inversion.

A noticeable feature during all three cruises – that was not mentioned earlier – was the patchiness and clustering of drizzle cells. During EPIC 2001, the scanning C-band radar was used to map the mesoscale organization (15-40 km) of the drizzle events (Comstock et al. 2005), although smaller scale variability within these mesoscale structures was observed as well. The horizontal extent of these drizzle cells as observed by the vertically pointing radar was between 2 and 5 km. Such individual drizzle cells were observed in larger mesoscale clusters in all cruises. This organization was observed under overcast conditions (EPIC 2001), broken stratus cloud conditions (Stratus 2003) and decoupled conditions with two distinct cloud bases (Stratus 2004). This hints the presence of a mesoscale convection organization imbedded in the larger-scale dynamics.

5.2 Outlook and Future Work

The persistence of marine stratus through the year and their extensive coverage makes these shallow marine clouds a significant component of the earth radiation budget. The systematic analysis and comparison of the ship-based observations of clouds and MABL properties provided a wealth of information for additional modeling and field studies. The documentation of the temporal and spatial variability of the MABL and clouds in the SE Pacific is an important step in understanding the physical processes that contribute to

the formation, maintenance and dissipation of marine stratocumulus. Radiative, microphysical and dynamical processes are coupled in a manner that complicates their representation in numerical models. These processes (e.g., turbulence, entrainment) act at small scales and the details of the physics that govern cloud lifecycle and drizzle formation are little understood. These processes need to be well observed and understood before an improvement in the parameterization of marine stratus clouds in Global Climate Models is achieved.

Our current understanding of the stratocumulus-capped boundary layer in the SE Pacific comes from the well-explored dataset obtained during the EPIC 2001 Stratocumulus study; due to the lack of additional observations up to the end of 2003, scientists – naturally – drew many conclusions based only on the particular dataset. The EPIC field experiment and its findings will always be a milestone for the SE Pacific stratocumulus regime that had been previously exposed to very limited observations with in-situ instrumentation. Nevertheless, parameterization schemes, model evaluations and general assessments based exclusively on these findings may be valid only for specific cases/time periods and may not hold for the entire domain of boundary layer-cloud interactions all-year round. For instance, prior to the Stratus 2003 research cruise (Kollias et al. 2004), the well-mixed conditions observed throughout the EPIC study were thought to be the primary mode of the boundary layer structure in the area during the Southern Hemisphere spring months. The 2003 and 2004 cruises though revealed many differences and a far more complex picture with respect to the EPIC findings, especially for boundary layer structure and evolution, even for the same spatial domains (WHOI buoy location) and for adjacent months (October-November-December). This highlights the

need for more in-situ observations and enhanced monitoring of the SE Pacific cloud-topped boundary layer, as well as the need for analysis of data from all research cruises already conducted in the area for boundary-layer-, cloud- and precipitation-related studies. Additional case studies with the use of the relatively new datasets would definitely help to better constraint and explain the documented variability that characterizes boundary layer structures and cloudiness in the area.

Some of the results obtained in this study can be directly correlated to satellite data for the SE Pacific area or model parameterizations for boundary layer structures and processes. A deeper analysis of the data should reveal even more interesting features, and could be used for evaluating specific satellite products and boundary-layer model simulations. Moreover, this dataset, including three successful observational periods over the span of four years, can be a reference point for the SE Pacific stratocumulus and could be ideally used for various intercomparisons with the better-studied stratus and stratocumulus clouds of the NE Pacific.

During the cruises, the air-sea flux system and the high temporal-resolution soundings provided adequate description of the MABL structure and evolution. However, the millimeter wavelength radars used on board the research vessels as part of the cloud observation systems were not compensated for ship motion and often saturated in the presence of heavy drizzle events (Ghate et al. 2005). Thus, besides the cloud reflectivity that can be used for the retrieval of the cloud boundaries and to classify the cloud observations in drizzling and drizzle-free periods, the Doppler measurements are not suitable for the retrieval of cloud dynamics and microphysics. In addition, no instrument-based method exists currently for the measurement of drizzle rain rates at the surface, and

the LWP measurements are often susceptible to biases and uncertainties (Zuidema et al. 2005). Finally, comprehensive measurements of aerosol mass distribution and chemistry are required for a better understanding of cloud-aerosol interaction.

A combination of millimeter wavelength cloud radars (35- and 94-GHz) from various platforms (e.g., island-based, ship-based and airborne) along with in-situ measurements of cloud microphysics and aerosols from aircraft penetrations in the context of a large field experiment in the near future could improve our understanding on marine stratus. Millimeter wavelength cloud radars have been used extensively the last 15 years for the study of boundary layer clouds. Using observations from a 35-GHz radar during the Atlantic Stratocumulus Transition Experiment (ASTEX; 1992), Miller and Albrecht (1995) study the diurnal cycle of the cloud structure of marine stratocumulus and Frisch et al. (1995a; 1995b) develop turbulence and microphysical retrieval techniques using airborne radar observations. Recently, Stevens et al. (2003) used airborne in-situ and radar observations to further examine the physics and dynamics of marine stratus off the coast of California. Currently the NOAA ESRL/PSD (formerly known as NOAA/ETL) is developing a 94-GHz radar with Doppler spectra capability and motion compensation for ship-based observations of boundary layer clouds. Such new and exciting tools or the use of a second radar frequency (e.g., X-band) could be used to retrieve the turbulent and microphysical structure of marine stratus. Such ship-based observations in the context of a large field experiment and the presence of aircraft in-situ measurements could lead to the generation of new datasets and better understanding of marine stratus.

APPENDIX

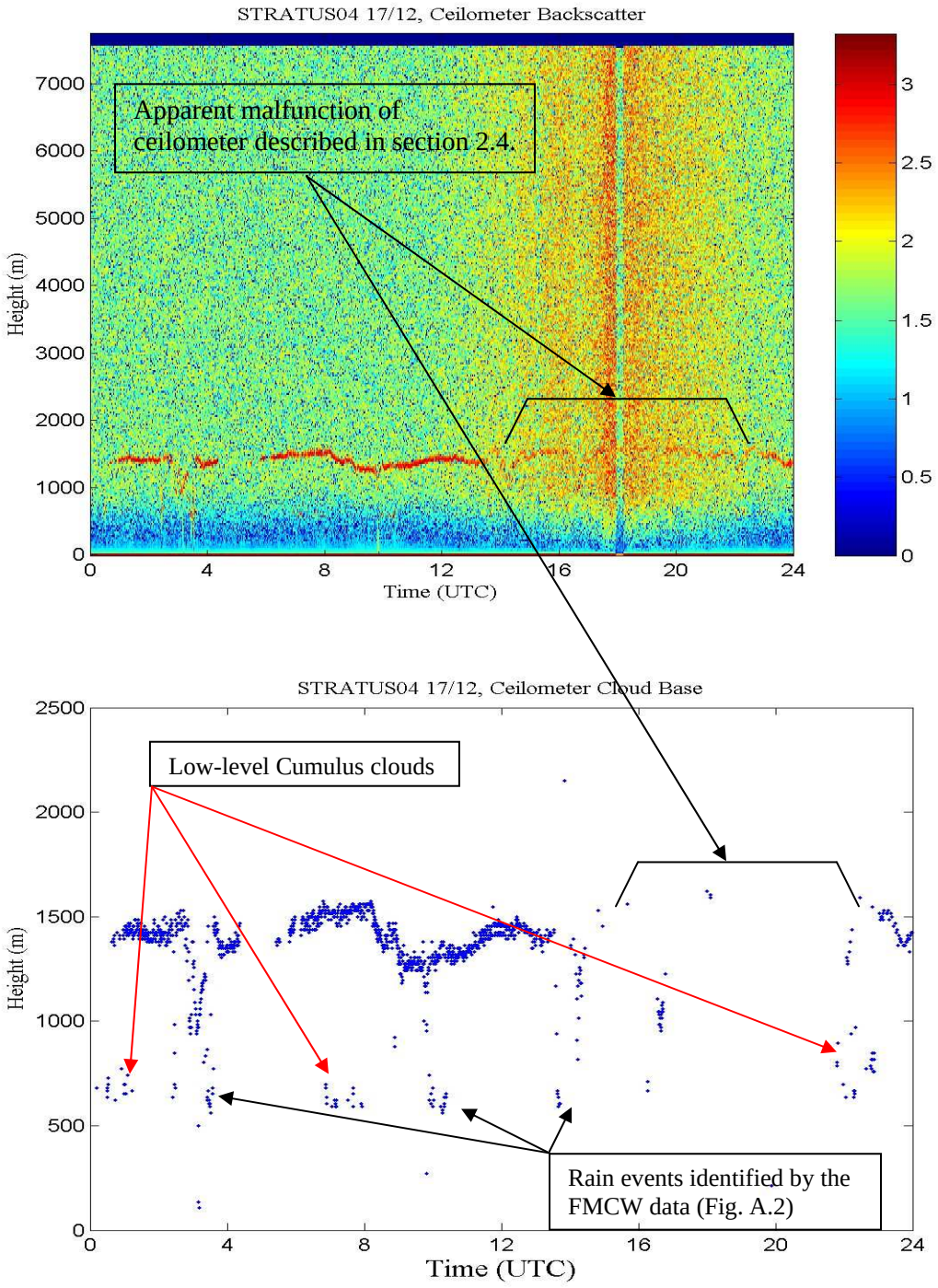

Figure A1: Ceilometer backscatter intensity (upper panel) and cloud base height (lower panel) for December 17, 2004.

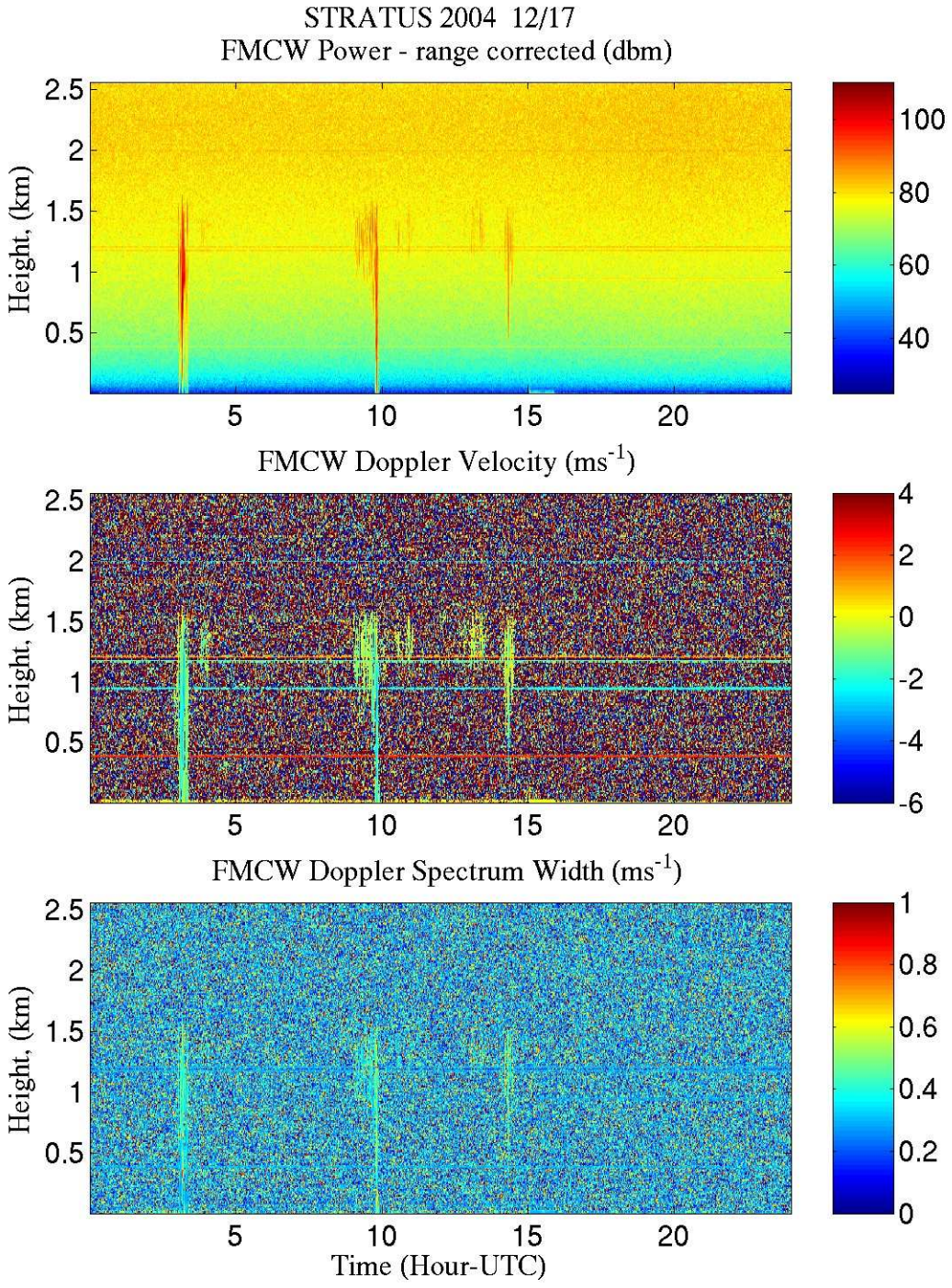

Figure A2: The three Doppler moments derived from the FMCW radar for December 17, 2004.

BIBLIOGRAPHY

Albrecht, B. A., 1989: Aerosols, cloud microphysics and fractional cloudiness. *Science,* **245,** 1227–1230.

——, D. A. Randall, and S. Nicholls, 1988: Observations of marine stratocumulus during FIRE. *Bull. Amer. Meteor. Soc*., **69,** 618–626.

——, M. P. Jensen, and W. J. Syrett, 1995a: Marine boundary layer structure and fractional cloudiness. *J. Geophys. Res.,* **100,** 14209–14222.

——, C. S. Bretherton, D. Johnson, W. H. Schubert, and A. S. Frisch, 1995b: The Atlantic stratocumulus transition experiment—ASTEX. *Bull. Amer. Meteor. Soc.,* **76,** 889–904.

Bolton, D., 1980: The computation of equivalent potential temperature. *Mon. Wea. Rev.,* **108,** 1046–1053.

Bougeault, P., 1985: The diurnal cycle of the marine stratocumulus layer: A higher-order model study. *J. Atmos. Sci.,* **42,** 2826–2843.

Bretherton, C. S., and M. C. Wyant, 1997: Moisture transport, lower tropospheric stability, and decoupling of cloud-topped marine boundary layers. *J. Atmos. Sci.,* **54,** 148–167.

——, T. Uttal, C. W. Fairall, S. Yuter, R. Weller, D. Baumgardner, K. Comstock, R. Wood, and G. Raga, 2004: The EPIC 2001 stratocumulus study. *Bull. Amer. Meteor. Soc.,* **85,** 967–977.

Clothiaux, E. E., M.A. Miller, B.A. Albrecht, T.P. Ackerman, J. Verlinde, D.M. Babb, R.M. Peters and W.J. Syrett, 1995: An evaluation of a 94-GHz radar for remote sensing of cloud properties. *J. Atmos. Oceanic Technol.,* **12,** 201–229.

Comstock, K. K., C. S. Bretherton, and S. E. Yuter, 2005: Mesoscale variability and drizzle in southeast Pacific stratocumulus. *J. Atmos. Sci.,* **62,** 3792–3807.

Fairall, C. W., A. B. White, J. B. Edson, and J. E. Hare, 1997: Integrated shipboard measurements of the marine boundary layer. *J. Atmos. Oceanic Technol.,* **14,** 338–359.

Frisch, A.S., C.W. Fairall and J.B. Snider, 1995a: Measurement of stratus cloud and drizzle parameters in ASTEX with a K_α–band Doppler radar and microwave radiometer. *J. Atmos. Sci*., **52,** 2788–2799.

Frisch, A. S., D.H. Lenschow, C.W. Fairall, W.H. Schubert and J.S. Gibson, 1995b: Doppler radar measurements of turbulence in marine stratiform cloud during ASTEX. *J. Atmos. Sci.,* **52,** 2800–2808.

Garreaud, R. D., and R. Muñoz, 2004: The diurnal cycle in circulation and cloudiness over the subtropical southeast Pacific: A modeling study. *J. Climate,* **17,** 1699–1710.

Garreaud, R. D., and R. C. Munoz, 2005: The low-level jet off the west coast of subtropical South America: Structure and variability. *Mon. Wea. Rev.,* **133,** 2246–2261.

——, J. Rutllant, J. Quintana, J. Carrasco, and P. Minnis, 2001: CIMAR-5: A snapshot of the lower troposphere over the subtropical southeast Pacific. *Bull. Amer. Meteor. Soc.,* **82,** 2193–2207.

Ghate, V. P., I. Jo, E. Serpetzoglou, B. A. Albrecht, P. Kollias, and J. B. Mead, 2005: High resolution observations of drizzle from stratocumulus using a 95-GHz FMCW radar. *Extended Abstracts, 32nd Conf. on Radar Meteorology,* Albuquerque, NM, Amer. Meteor. Soc., CD-ROM, P1R.1.

Kalnay, E. and Coauthors, 1996: The NCEP/NCAR Reanalysis 40-year project. *Bull. Amer. Meteor. Soc.,* **77**, 437–471.

Klein, S. A., and D. L. Hartmann, 1993: The seasonal cycle of low stratiform clouds. *J. Climate,* **6,** 1587–1606.

Kloesel, K. A., and B. A. Albrecht, 1989: Low-level inversions over the tropical Pacific—thermodynamic structure of the boundary layer and the above-inversion moisture structure. *Mon. Wea. Rev.,* **117,** 88–101.

Kollias P., and B. A. Albrecht, 2000: The turbulence structure in a continental stratocumulus cloud from millimeter-wavelength radar observations. *J. Atmos. Sci.,* **57,** 2417–2434.

Kollias P., C. W. Fairall, P. Zuidema, J. Tomlinson, and G. A. Wick, 2004: Observations of marine stratocumulus in SE Pacific during the PACS 2003 cruise. *Geophys. Res. Lett*., **31**, L22110

Li, T., and S. G. H. Philander, 1996: On the annual cycle of the eastern equatorial Pacific. *J. Climate,* **9,** 2986–2998.

Miller, M.A., and B.A. Albrecht, 1995: Surface-based observations of mesoscale cumulus-stratocumulus interaction during ASTEX. *J. Atmos. Sci.,* **52**, 2809–2826.

Minnis, P., P. W. Heck, D. F. Young, C. W. Fairall, and J. B. Snider, 1992: Stratocumulus cloud properties derived from simultaneous satellite and island-based instrumentation during FIRE. *J. Appl. Meteor.*, **31,** 317–339.

Pyatt, H. E., B. A. Albrecht, C. Fairall, J. E. Hare, N. Bond, P. Minnis, and J. K. Ayers, 2005: Evolution of marine atmospheric boundary layer structure across the cold tongue-ITCZ complex. *J. Climate,* **18,** 737–753.

Ramanathan, V., R. D. Cess, E. F. Harrison, P. Minnis, B. R. Barkstrom, E. Ahmad and D. Hartmann, 1989: Cloud-radiative forcing and climate: Results from the Earth Radiation Budget Experiment. *Science,* **243,** 57–63.

Randall, D. A., J. A. Coakley, C. W. Fairall, R. A. Kropfli, and D. H. Lenschow, 1984: Outlook for research on subtropical marine stratiform clouds. *Bull. Amer. Meteor. Soc*., **64,** 1290–1301.

Rozendaal, M. A., and W. B. Rossow, 2003: Characterizing some of the influences of the general circulation on subtropical marine boundary layer clouds. *J. Atmos. Sci.*, **60,** 711–728.

Rutllant, J.**,** 1993: Coastal lows and associated southerly winds in north-central Chile. Preprints, *Fourth Int. Conf. on Southern Hemisphere Meteorology,* Hobart, Australia, Amer. Meteor. Soc., 268–269.

Serpetzoglou, E., C. W. Fairall, D. E. Wolfe, V. P. Ghate, I. Jo, B. A. Albrecht and P. Kollias, 2005: Properties of the SE Pacific stratocumulus using mm-wave radars and other remote sensors. *Extended Abstracts, 32nd Conf. on Radar Meteorology,* Albuquerque, NM, Amer. Meteor. Soc., CD-ROM, 2R.2.

Stevens, B., and Coauthors, 2003: Dynamics and chemistry of marine stratocumulus—DYCOMS-II. *Bull. Amer. Meteor. Soc.*, **84,** 579–593.

Weller, R., cited 1999: A science and implementation plan for EPIC. [Available online at http://www.atmos.washington.edu/gcg/EPIC/EPIC_rev.pdf]

Wood, R., and C. S. Bretherton, 2004: Boundary layer depth, entrainment, and decoupling in the cloud-capped subtropical and tropical marine boundary layer. *J. Climate,* **17,** 3576–3588.

——, ——, and D. L. Hartmann, 2002: Diurnal cycle of liquid water path over the subtropical and tropical oceans. *Geophys. Res. Lett.,* **29,** 2092, doi:10.1029/2002GL015371.

Yin, B., and B. A. Albrecht, 2000: Spatial variability of atmospheric boundary layer structure over the eastern equatorial Pacific. *J. Climate,* **13**, 1574–1592.

Zhang, C., M. McGauley, and N. A. Bond., 2004: Shallow meridional circulation in the tropical eastern Pacific. *J. Climate*, **17,** 133–139.

Zuidema, P., E. R. Westwater, C. Fairall, and D. Hazen, 2005: Ship-based liquid water path estimates in marine stratocumulus. *J. Geophys. Res.,* **110,** in proof, doi:10.1029/ 2005JD005833.